Water status in soil and crops

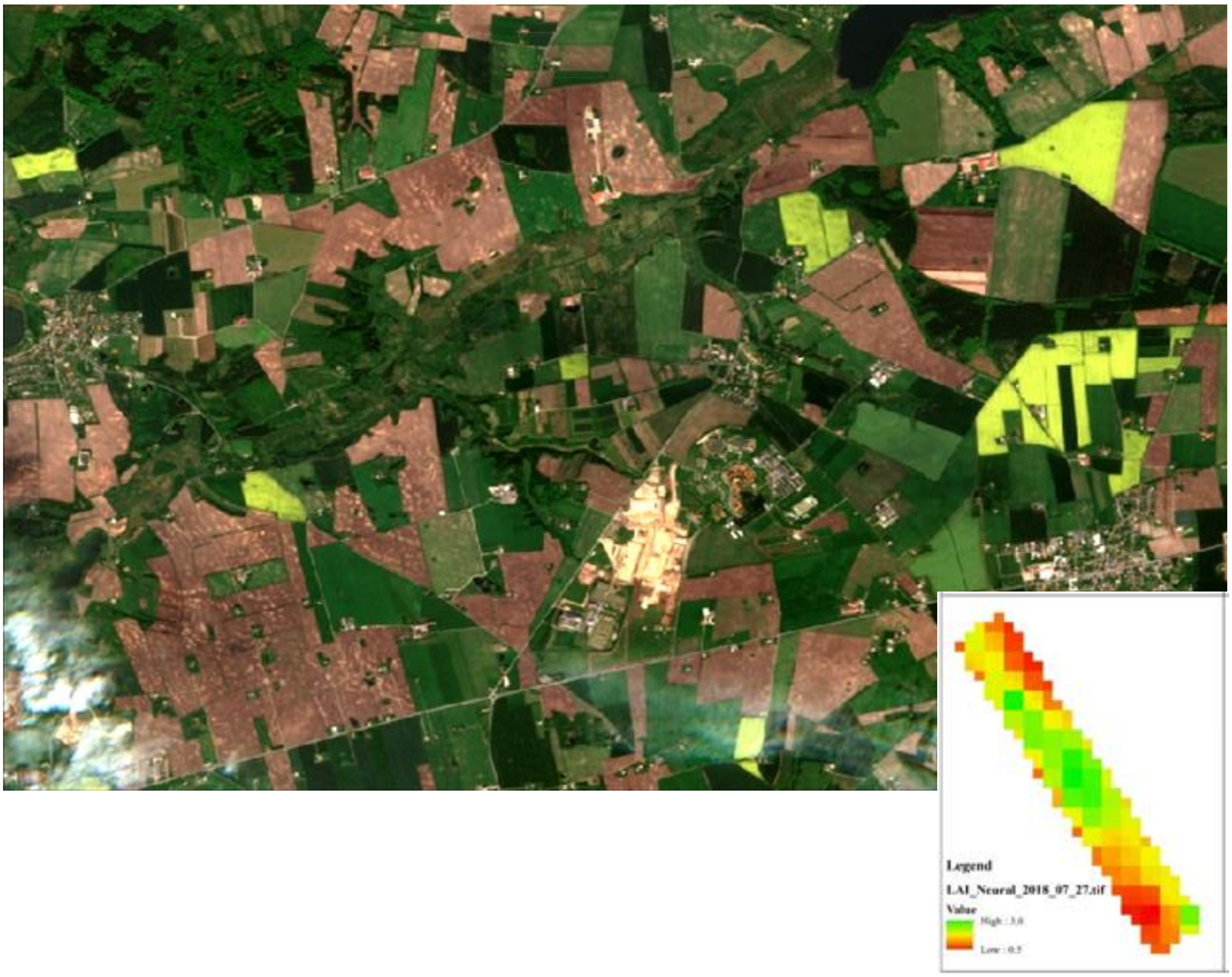

Junxiang Peng, Katarzyna Dorota Gielnik, Loraine ten Damme, Kiril Manevski, Emmanuel Arthur
Mogens H. Greve, Mette Greve, Kirsten Kørup Sørensen, Mathias Neumann Andersen

Department of Agroecology, Aarhus University

30-1-2019

Den Europæiske Landbrugsfond for Udvikling af Landdistrikterne:
Danmark og Europa investerer i landdistrikterne

Miljø- og Fødevareministeriet
Landbrugsstyrelsen

Den Europæiske Landbrugsfond
for Udvikling af Landdistrikterne

LDP 2020

Se EU-Kommissionen, Den Europæiske Landbrugsfond for Udvikling af Landdistrikterne

Executive Summary

SEGES is in the process of re-programming the popular decision support system Vandregnskab for use in a wider suite of applications where water balances are required. In connection with this, the program should be opened up for acquiring data from the many new sources that are foreseen to become available in the near future from sensors and satellites. The present report is looking into some of these areas by describing a method to calculate leaf area index (LAI) from satellite images as LAI is a key variable in the crop and water balance model. Furthermore, the calculation of root zone capacity for individual fields should be more precise taking advantage of new soil database information and estimates of rooting depth of crops. Furthermore, a range of 'new' crops have entered the agricultural field in later years, as catch crops and undersown crops are widely used as a means of reducing nitrogen leaching. These need to be included and parameters derived for LAI development modelling in Vandregnskab. Finally, the Vandregnskab model needs to give better estimates of yield response to water both for supporting tactical decisions on irrigation throughout the season in mixed rotations and for strategical decisions on investments in irrigation facilities. To that end, a number of crop water production functions have been parameterized and need to be implemented in the model.

In the report we describe a test of a neural network model to calculate LAI from satellite multispectral images. The reflectances measured by the satellite were compared to ground measurements taken in an irrigation experiment with potatoes at AU with large plots of 30 x 30 m. The reflectances were shown to have little correspondence between satellite and ground measurements, when looking at the individual bands that are normally used to derive LAI estimates from vegetation indices. Nevertheless, when deriving LAI values from the satellite data, we obtained excellent correspondence between two fundamentally different methods, with results which look reasonable and presumably can be further enhanced.

An experiment with three years of data on growth of catch crops at AU-Foulum was used for fitting new models (parameters) for the general LAI development model of Vandregnskab. An algorithm in R was developed to derive LAI from reflectance measurements.

Optimizations of the calculation procedure for individual fields with respect to root zone capacity is described. Rather than being based on classification of the soil type and using a standard figure for each soil type the root zone capacity should be calculated directly from texture using pedotransfer functions. Improved soil database information and better estimates of rooting depth should further add to the precision of the estimates.

For the crop water production funtions used to estimate yield response to irrigation, a model profiling the drought sensitivity of a crop throughout the season has been developed. By use of historical yield results from irrigation experiments in Denmark, the model has been parameterized for 12 different main agricultural crops, which is a sizeable expansion compared to previous. The models for the different crops can be used to prioritize in-season irrigation at farm level in case of limited irrigation capacity. Furthermore, we have simulated unirrigated yield of 10 crop species during 26 years (1990-2015) at 10 locations and at 6 root zone capacities in order to derive the average yield increases that can be expected when going from unirrigated to irrigated conditions. Such calculation are of fundamental importance for decions on investment in irrigation facilities.

.

Index: **Page**

Satellite data as input to water balance model: Estimation of leaf area index using Sentinel 2 imagery

Junxiang Peng, Kiril Manevski, Kirsten Kørup Sørensen, Mathias Neumann Andersen
Department of Agroecology, Aarhus University, Blichers Allé 20, 8830 Tjele, Denmark

Abstract: In this research, two different methods to estimate leaf area index (LAI) of potatoes were evaluated. These were 1) a neural network training model and 2) calculation of intercepted radiation and conversion to LAI. Nondestuctively sampled ground measurement data of reflectance (Rapidscan instrument) and LAI (LAI-2000 instrument) was used to validate the results derived from satellite image processing. The result showed that the reflectance values for similar wavelength bands of satellite and rapidscan did not correlate well (R^2, 0.54), and the LAI estimated from two ways did not fit well with the local measurement LAI data (R^2, 0.34). Maybe more ground measurements or using higher resolution imagery can solve this problem. Nevertheless, the LAI estimated from two methods correlated well as the R^2 value wass 0.89 (p<0.001), which indicate that both models can be used to measure LAI after validation.

Key words: leaf area index; Sentinel 2; neural network training; Fractional interception of photosynthetically active radiation

Background

Leaf area index (LAI), defined as the ratio between the sum of the foliar area and the unit of soil surface (Watson, 1947), is a key variable for characterizing differences between plant canopies and in turn plant growth because it is related to light and energy capture (Ramírez-García et al., 2012). Due to the importance of this index, many methods to measure it have been developed. Generally, the methods can be categorized in two main groups, direct methods and indirect methods (Breda, 2003). The direct methods encompass destructive sampling of the vegetation within a delimited surface area and measuring the leaf area. There are various methods to measure the leaf area, for instance, measuring the area of all of the leaves with scanners or imageprocessing, or converting the dry mass of the leaves to LAI by multiplying it with some parameters e.g. specific leaf area (SLA, $cm^2\ g^{-1}$) as described by Breda (2003).However, the shortcomings are obvious. It is destructive, time consuming, and not suitable for large-scale field measurements. Therefore, indirect methods were developed in which the LAI value can be estimated from measurements of the transmission of radiation through the canopy, based on the radiative transfer theory (Monteith and Ross, 1981). It is non-destructive and the idea is using gap fraction, leaf angle, and zenith angle to estimate the LAI (Breda, 2003). Nowadays, LAI-2000 (Li-Cor, Lincoln, Nebraska, USA) is one of the popular instruments to measure the LAI. It measures in five zenith angles simultaneously, ranging from 0° to 75° through a fish-eye light sensor, that observes diffuse radiation transmission through the canopy. The measured gap fraction data are inverted to obtain the effective LAI under the assumption of a random spatial distribution of leaves (Chen et al., 2002). Measurements are taken below and above the canopy .Even though the indirect method, represented by LAI-2000, is a non-destructive and relative easy way to measure the LAI, it doesnot entire solve the problems encountered by the direct methods, as it is still time consuming and not very effective for large scale field measurements.

Starting from the 1990s, satellite images were used to estimate the leaf area index. The most common method was to estimate the relationship between the indices calculated from the satellite imagery (like NDVI) and ground-measured LAI and then using the equation derived from the relationship to calculate the LAI from the satellite imagery. For instance, Chen and Cihlar. (1996)

used landsat TM images to estimate LAI of boreal conifer forest by correlating the NDVI and RVI with the ground measured LAI in Canada (Chen and Cihlar, 1996). Colombo *et al.* (2003) used high geometric resolution (1-m spatial resolution) imagery acquired from the IKONOS satellite to compute different spectral vegetation indices (SVIs) and utilized the relationship estimated from SVIs with the ground-measured LAI to calculate the LAI for different plants in Italy (Colombo et al., 2003).Besides direct calculation of LAI from the satellite imagery indices based on correlation, another important parameter, the fraction of intercepted photosynthetically active radiation (Fipar) was derived and used to compute LAI based on their relationship. For instance, Asrar *et al*. (1984) used an empirical formula to calculate Fipar and in turn LAI from NDVI values derived from spectral data for wheat in US (Asrar et al., 1984). Andersen *et al*. (1996) utilized Fipar calculated from measured reflectance ratio to estimate the effect of drought and nitrogen on growth and yield of winter oilseed rape in Denmark.This was based on the article by Christensen and Goudriaan (1993), who developed a method to retrieve Fipar based on the reflectance ratio (RVI) and then used the Fipar to estimate the biomass of spring barley. Afterwards, this method has also been cited and utilized by scientists in the field of ecosystem research. For instance, Manevski *et al*. (2017) estimated the radiation use efficiency and biomass of perennial grasses in Denmark (Manevski et al., 2017). Based on the theorethical relationship between RVI, Fipar and LAI, the LAI can be estimated from the reflectance measurements (e.g. Campbell, 1977).

From 2000s, with the utilization of the computer deep learning, inversion methods for physically-based models and its application neural network training method were used to approximate an input-output relation or a mapping function between a canopy's spectral reflectance and its structural and optical parameters. The basic assumption is that the spectral reflectance of a canopy is a function of the geometry and characteristics of its constituent elements (e.g., tree height, size), the spatial distribution of the elements, and the illumination and viewing geometry (Kimes et al., 2000). Based on this idea, Bacour et al. (2006) used the SAIL (Verhoef, 1985) and PROSPECT (Jacquemoud and Baret, 1990) models to simulated 11 reflectance based on the nine setting biophysical parameters. The parameters contained leaf structure parameters, chlorophyll content(a,b), the equivalent water thickness, the dry matter content, the brown pigment concentration, multiplicative brightness parameter, leaf area index, leaf inclination angle, hot spot parameter, vegetation cover. After the simulation and training the neural network, based on the inversion idea, the biophysical parameters were estimated by the satellite reflectance imagery (Bacour et al., 2006). On 02/05/2016, French National Institute for Agricultural Research (INRA) released the first version of toolbox, which was installed in the Sentinel application platform (Marie Weiss, 2016). https://step.esa.int/docs/extra/-ATBD_S2ToolBox_L2B_V1.1.pdf. The neural network was established by feeding sets of biophysical variables and after the training of the neural network, the biophysical parameters can be estimated from the reflectance by inversed modelling using the neural network model (Fig. 1).

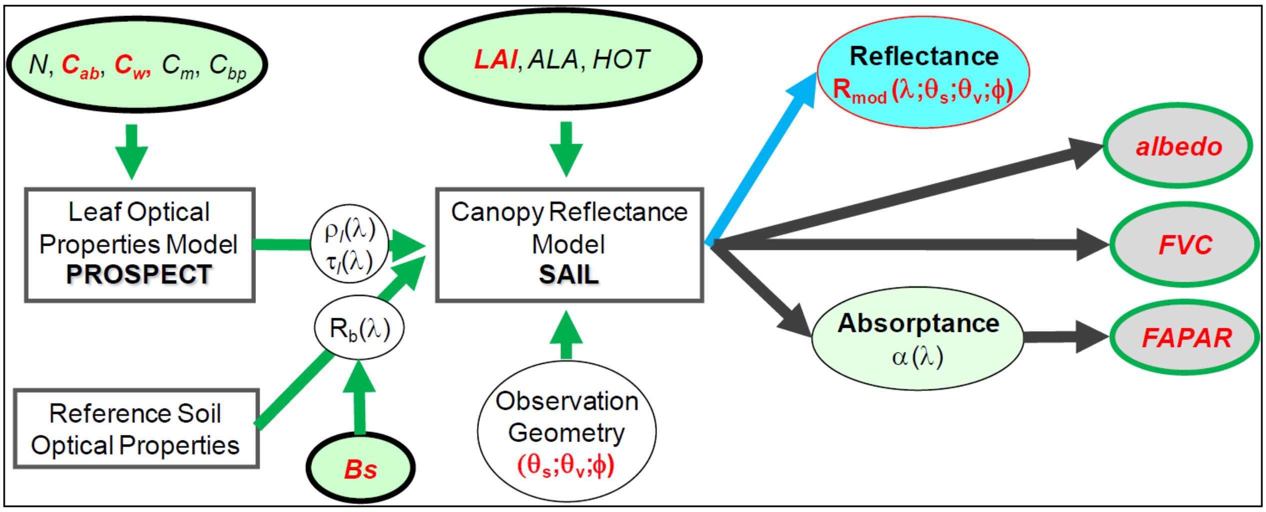

Figure 1. The coupled PROSPECT+SAIL model to generate the training database made of TOC reflectance and corresponding biophysical variables. (modified from Fig. 4, Marie Weiss, 2016)

In the the current study we focus on estimation of LAI from satellite imagery based on two different methods, from Fipar calculated from reflectance measurements, and from neural network training and estimation. After the LAI have been estimated by the two methods, comparison will be done to judge the relative merits of the two methods.

Materials and Methods

Research location

Field experiments was conducted from May to November in 2018 in Denmark. The location of the experimental field is Havrisvej 20, 8830 Tjele on coarse sand, Danish soil classification JB 1 (sandy) (56°31'59.6''N 9°24'39.4''E). The annual precipitation is 726 mm and average temperature is 7.6 degree Celsius (1901-2015). The experimental crop is starch potato (*Solanum tuberosum* cv. Oleva). The field experiment has 24 plots with six different combinations of fertilization and irrigation treatments and 4 replications. The objective of the experiment was to manage and optimize the fertilization and irrigation by satellite imagery analysis.

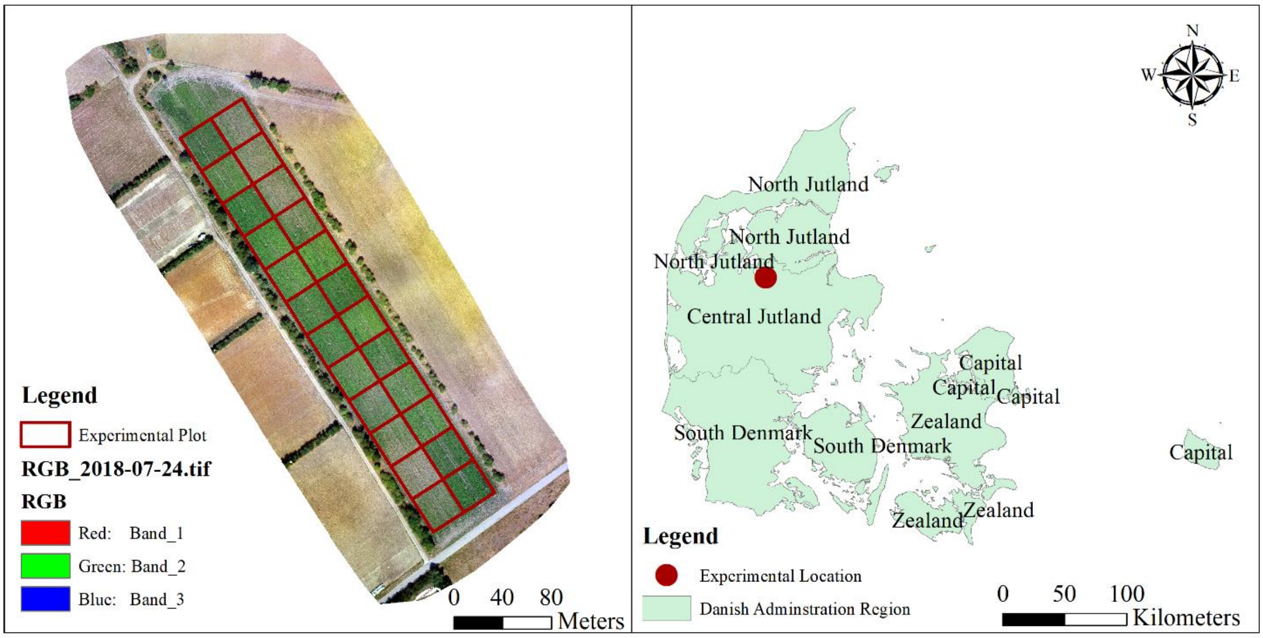

Figure 2. Location of experimental field (in the left, the RGB image was UAV image got from 24th July, and the red plot means the experimental designed plots.).

LAI estimation algorithm

Neural network training

As described above, the basic idea of this method is to use the coupled PROSPECT+SAIL model to generate the training database made of reflectance imagery and corresponding biophysical variables. The biophysical parameters can be estimated from the reflectance by inversion using the neural network model. The input set biophysical variables contain leaf mesophyll structure index, Leaf chlorophyll content, Leaf dry matter content, Leaf water content, Leaf brown pigment content, Leaf area index, average leaf angle, hot spot parameter and brightness parameter (Table 1).

Table 1 Distribution of the input variables of the radiative transfer model used to generate the training data base (modified from table 5 from (Marie Weiss, 2016)).

Dimension	Variable	Abbreviation	Min	Max	Mode	Std	Nb_Class	Law
Canopy	Leaf Area Index	LAI	0.0	15.0	2.0	3.0	6	Gauss
	Average Leaf Angle	ALA(°)	30	80	60	30	3	gauss
	Hot Spot Parameter	Hot	0.1	0.5	0.2	0.5	1	gauss
Leaf	Leaf Mesophyll Structure Index	N	1.20	2.20	1.50	0.30	3	gauss
	Leaf Chlorophyll Content	Cab($\mu g.m^{-2}$)	20	90	45	30	4	gauss
	Leaf Dry Matter Content	Cdm($g.m^{-2}$)	0.0030	0.0110	0.0050	0.0050	4	gauss
	Leaf Water Content	CW_Rel	0.60	0.85	0.75	0.08	4	uni
	Leaf Brown Pigment Content	Cbp	0.00	2.00	0.00	0.30	3	gauss
Soil	Brightness Parameter	Bs	0.50	3.50	1.20	2.00	4	gauss

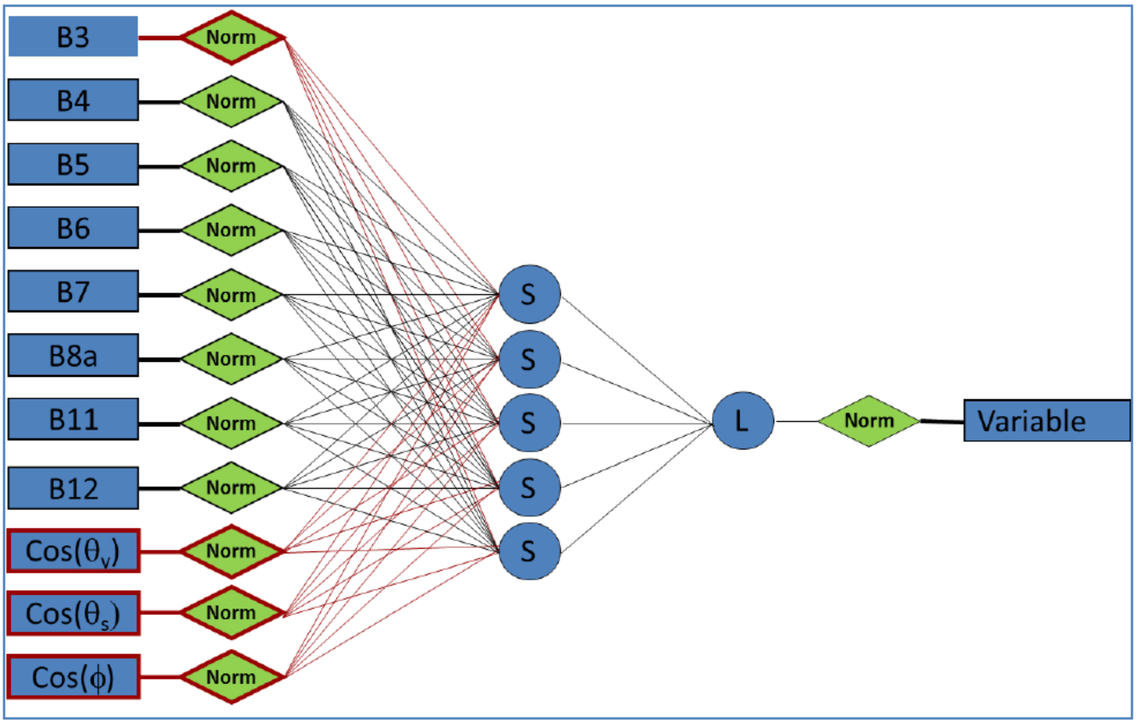

Figure 3. Neural network architecture developed for the estimation of the biophysical variables considered from the 8 SENTINEL2 bands and the 3 angles defining the geometry of observation. The network is made of 1 hidden layer of 5 neurons and 1 linear output neuron. The 'Norm' symbols correspond to the normalization process. Symbols 'S' and 'L' correspond respectively to the sigmoid (tansig) and linear transfer functions of the neurons (cited from Marie Weiss (2016)) .

After the training of the neural model based on the input variables, the eight sentinel bands data will be input to the model after the normalization process. With the re-running the model, the biophysical indices, like LAI, FAPAR (fraction of absorbed photosynthetically active radiation), and FCOVER (vegetation cover fraction) can be derived after the normalization process (Fig. 3).The calculation algorithm behind this neural training model can be found from the two references of SAIL (Verhoef, 1985) and PROSPECT (Jacquemoud and Baret, 1990).

LAI estimated by Fipar calculated from RVI

Christensen and Goudriaan developed the equations that estimate RVI from Fipar and vice versa (Christensen and Goudriaan, 1993). The equation is:

$$RVI = \frac{\left[\rho_{IR,\infty}+\left(\frac{\eta_{NIR}}{\rho_{NIR,\infty}}\right)(1-f_{ipar})\right](1+\eta_R(1-f_{ipar})^2)}{\left[\rho_{R,\infty}+\left(\frac{\eta_R}{\rho_{R,\infty}}\right)(1-f_{ipar})^2\right](1+\eta_{NIR}(1-f_{ipar}))} \quad (1)$$

$$\eta_j = (\rho_{j,\infty} - \rho_{j,s})/(\rho_{j,\infty} - 1/\rho_{j,\infty}) \quad (2)$$

Where, $\rho_{j,\infty}$ indicates the reflectance of the red (R) and near infrared (NIR) at high LAI (LAI>8), and $\rho_{j,s}$ is the reflectance of bare soil at the selected wavelength (*j*).Since RVI and LAI has non-linear positive relationship (Zhou et al., 2017), we assumed that RVI will also be high where the LAI is high, so that we used reflectance of the red (R) and near infrared (NIR) at highest RVI to calculate $\rho_{j,\infty}$ and $\rho_{j,s}$.

Due to the equation (1) is non-linear nature function, it is not possible to use this equation to calculate Fipar from RVI. Therefore a approximate power function was fitted to calculate Fipar based on RVI (Manevski et al., 2017). The equation is:

$$Fipar = a + bRVI^{C} \qquad (3)$$

Where RVI is calculated by Eq. (1), and a, b and c are iteratively fitted parameters with initial values of usually 1. The optimization of a, b and c was done by iteration using the optimization algorithm in the family of quasi-Newton methods that approximates the Broyden–Fletcher–Goldfarb–Shanno (BFGS) algorithm using a limited amount of computer memory by machine learning (Malouf and Groningen, 2009). This step was conducted by Optim function in R (R.3.5.1) that minimized the sum of squared deviation between Fipar from Eq. (3) and (1). Once the optimal values of a, b and c were found, Fipar may be calculated according to Eq. (3) using the RVI calculated from satellite imagery based on the following equation:

$$RVI = \frac{\rho_{NIR}}{\rho_R} \qquad (4)$$

Where, ρ_{NIR} and ρ_R means reflectance at near infrared and red bands.

If flat leaves in a canopy of leaf area index LAI, are randomly distributed in space, then the fraction of incident beam radiation from zenith angle that penetrates the canopy can be expressed as (Andersen et al., 1996; Campbell and Norman, 1998):

$$Fipar = 1 - \exp(-K \times LAI) \qquad (5)$$

where K is an extinction coefficient.

For a spherical leaf angle distribution, K can be estimated by taking the zenith angle of the sun (θ) into account (Campbell and Norman, 1998) as:

$$K = \frac{1}{2\cos(\theta)} \qquad (6)$$

Based on the assumption that potato has a spherical leaf angle distribution, LAI can be estimated by Fipar according to following equation:

$$LAI = -2\cos\theta \ln(1 - Fipar) \qquad (7)$$

In the current study, the zenith angle of the sun (θ) was calculated using zenith function in R (R 3.5.1) by input the latitude, longitude and satellite passing time in UTC format.

Measurements and Data Collection

The field measurement was performed weekly from 25/06/2018 to 05/09/2018. Ground canopy reflectance was measured by standard, handheld, 3-channel radiometer RapidSCAN CS-45 (Holland Scientific, Lincoln, Nebraska, USA). The sensor measure crop/soil reflectance at 670 nm, 730 nm and 780 nm simultaneously. Due to its internal modulated polychromatic light source, it is unaffected by ambient illumination allowing it to take accurate measurements no matter the weather conditionLAI-2000 (Li-Cor, Lincoln, Nebraska, USA) was used to measure the LAI under overcast conditions and followed the instruction manual for measuring in row crops. The radiation above and below the canopy were measure to calculate the gap fraction and compute the LAI.

Sentinel 2 (2A and 2B) imagery was downloaded from May to September from Europe Space Agency website (https://scihub.copernicus.eu/dhus/#/home). During this time, 60 days data were download, 22 days data were kept by removing the data, which was covered by clouds totally or partly. Sentinel 2 has twelve bands data with the different spatial resolution from 10 meters to 60 meters. Sentinel 2A and 2B are almost identical (Table 2) operating together to achieve frequent revisits and high mission availability.Sentinel-2 provide Level-0, Level-1 and Level-2 products. Level 0 data is compressed raw image data in Instrument Source Packet (ISP) format. Level 1 has two different kind of data format.

The Level-1A product is obtained by decompressing the Level-0 raw image data. Both level 0 and level 1A data are not available for users. The Level-1B product provides radiometrically corrected imagery at Top-Of-Atmosphere (TOA) radiance values and in sensor geometry. The Level-1C product is composed of Level-1B 100 km^2 tiles. The Level-2A product provides Bottom of Atmosphere (BOA) (or top of canopy TOC) reflectance images derived from the associated Level-1C products (cited from Sentinel 2 User Handbook: (https://sentinel.esa.int/documents/247904/685211/Sentinel-2_User_Handbook)

Table 2. Sentinel 2 bands and its wavelength, bandwidth and spatial resolution

Sentinel-2 bands	Sentinel-2A		Sentinel-2B		
	Central wavelength (nm)	Bandwidth (nm)	Central wavelength (nm)	Bandwidth (nm)	Spatial resolution (m)
Band 1 – Coastal aerosol	443.9	27	442.3	45	60
Band 2 – Blue	496.6	98	492.1	98	10
Band 3 – Green	560.0	45	559	46	10
Band 4 – Red	664.5	38	665	39	10
Band 5 – Vegetation red edge	703.9	19	703.8	20	20
Band 6 – Vegetation red edge	740.2	18	739.1	18	20
Band 7 – Vegetation red edge	782.5	28	779.7	28	20
Band 8 – NIR	835.1	145	833	133	10
Band 8A – Narrow NIR	864.8	33	864	32	20
Band 9 – Water vapour	945	26	943.2	27	60
Band 10 – SWIR – Cirrus	1373.5	75	1376.9	76	60
Band 11 – SWIR	1613.7	143	1610.4	141	20
Band 12 – SWIR	2202.4	242	2185.7	238	20

In the current research, the sentinel level 2A data from sentinel 2A and 2B was utilized to analyze. By matching the satellite date and ground measurement according to the time difference, 8 days of data were chosen to compare the satellite derived data and ground measurement data (Table 3).

Table 3. The matching of the satellite date and ground measurement date

Ground Measurement Date	Satellite Match Date	Time Difference (Days)
25-06-2018	27-06-2018	2
04-07-2018	02-07-2018	2
10-07-2018	09-07-2018	1
23-07-2018	24-07-2018	1
01-08-2018	27-07-2018	5
07-08-2018	08-08-2018	1
20-08-2018	21-08-2018	1
05-09-2018	02-09-2018	3

Statistical Analysis

The linear fitting model was used to evaluate the relationship between the satellite imagery reflectance value and ground measurement reflectance measurement, the LAI calculated from the satellite imagery and LAI measured in the field, and the LAIs estimated from two different methods.This was accomplished by using the lm function in R (R.3.5.1).In this report, LAI estimated by neural network model was performed by SNAP software (http://step.esa.int/main/toolboxes/snap/). The operation in SNAP to calculate the LAI is resample the different bands by Raster-Geometric Operations-Resampling, and then calculate the biophysical parameters by Optical-Thematic Land Processing-Biophysical Processor. Calculation of LAI from Fipar and the fitting of the linear model was conducted in R.3.5.1. Figures were plotted by using R.3.5.1 and ArcMap 10.4.

Results

Validation of the satellite reflectance data with the ground measurement data

The average value of the red and near infrared reflectance from two different platforms were similar (for satellite, the average value of red and near infrared reflectance were 0.05±0.01 and 0.37±0.07; for ground measurement from rapidscan, they were 0.05±0.03 and 0.38±0.03). However, if we look at the variation we can see that in the red band, data from rapidscan fluctuated more than those from the satellite; however, for the near infrared band, data from satellite fluctuated more than rapidscan data (Fig. 4). A linear fitting model was used to validate satellite data by ground measurement. The R^2 value of these two model were same, 0.54 (figure 5).

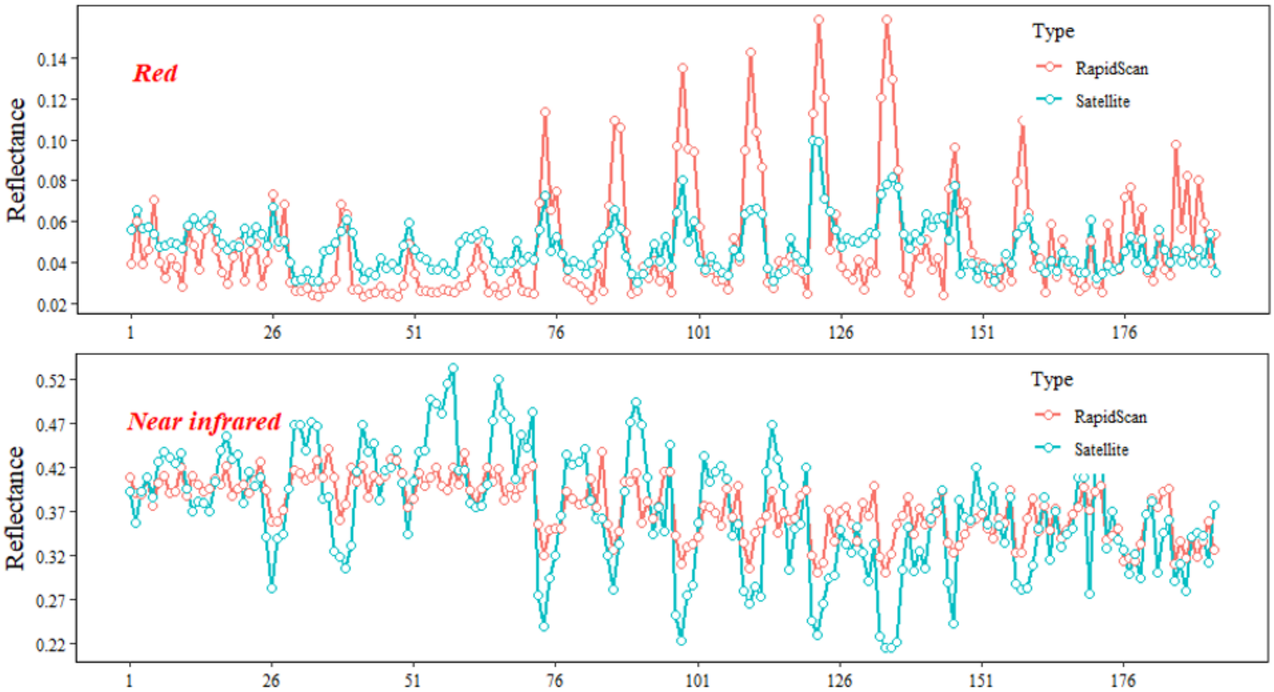

Figure 4. Temporal variation of the red reflectance measured by RapidScan and satellite. (x axis represents plot 1 to plot 24 ordered in a sequence starting on the first day of measurement (27/06/2018) and then with running numbers for each consequtive measurement date up to the last (02/09/2018))

Validation of the LAI estimated from satellite data using ground measurement data

The average value calculated from the LAI estimated from the neural network model and Fipar calculation were 1.69±0.54 and 1.25±0.67, respectively; however the average value measured in the field with LAI-2000 was 1.83±0.86. The ground measured LAI by using LAI-2000 instrument fluctuated more than the estimated LAI, which can be seen in Fig. 6.The linear fitting model was used to validate estimated LAI measured with LAI-2000 by ground measurement. The R^2 value of these two models were the same, 0.34.

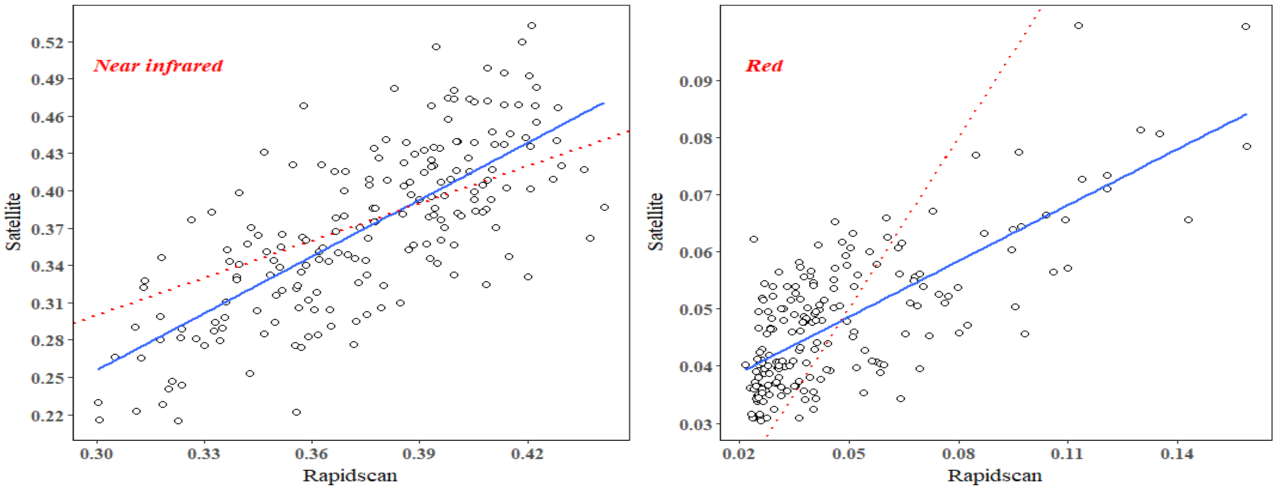

Figure 5. Validation of satellite reflectance. (Linear fitting model was used, the R^2 values for the two model are same, 0.54(p < 0.01). The stippled line in the plot is the 1:1 line.)

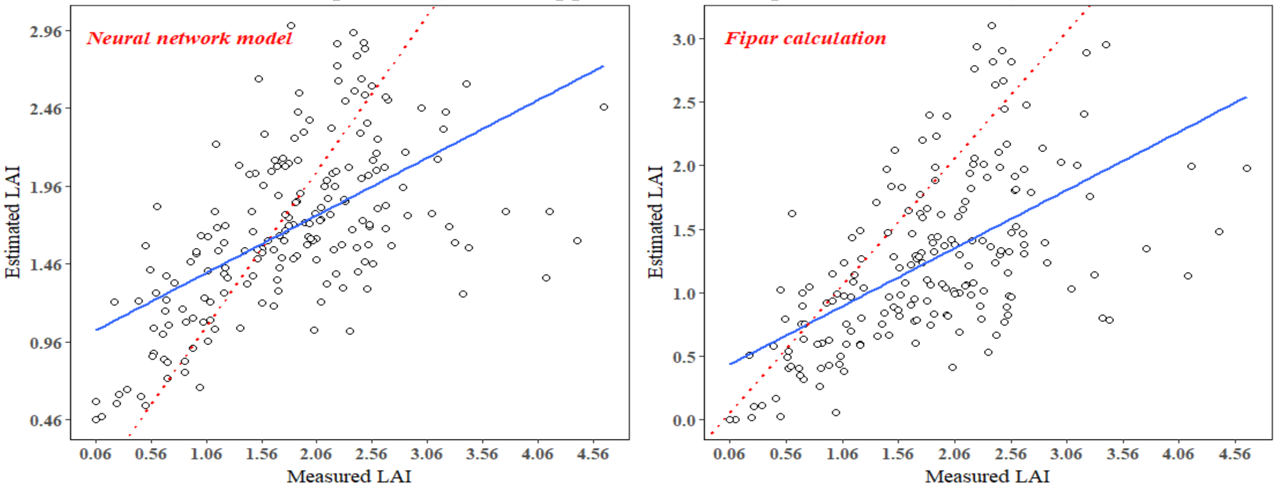

Figure 6. Validation of LAI estimated from neural network model and Fipar calculation against ground measured data with LAI-2000. Linear fitting model was used, the R^2 values for the two model are the same, 0.34 (p < 0.01). The stippled line in the plot is the 1:1 line.)

LAI derived from satellite

Based on the estimation and validation, the LAI was calculated by two different methods. The average LAI value of the whole season (22 days) estimated from neural network model (1.69) was higher than LAI estimated from Fipar calculation (1.25). The eight days that were chosen and used for the satellite data validation against ground measurement data are shown in Table 3. It can be easily seen from Fig. 7 and Fig. 8 that even though the spatial resolution is low for the small 30 x 30 m plots in the field, we can still distinguish the different treatments of the plots in the field. Unirrigated areas (with low LAI) were localized in the upper right and lower left corners of the field (Figs. 7 and 8)Daily average of LAI was calculated of the whole dataset comprising 22-days of data. The trend of the LAI estimates over the whole season was that LAI increased in the beginning reaching the peak value in the middle of the growing season, thereafter decreased significantly, as expected. Another phenomenon that can be noted,was that the LAI estimated from neural network model was higher than that estimated from Fipar calculation (Fig. 9). Even though both estimates seems rather on the low side, it has to be remembered that the average include unirrigated plots.

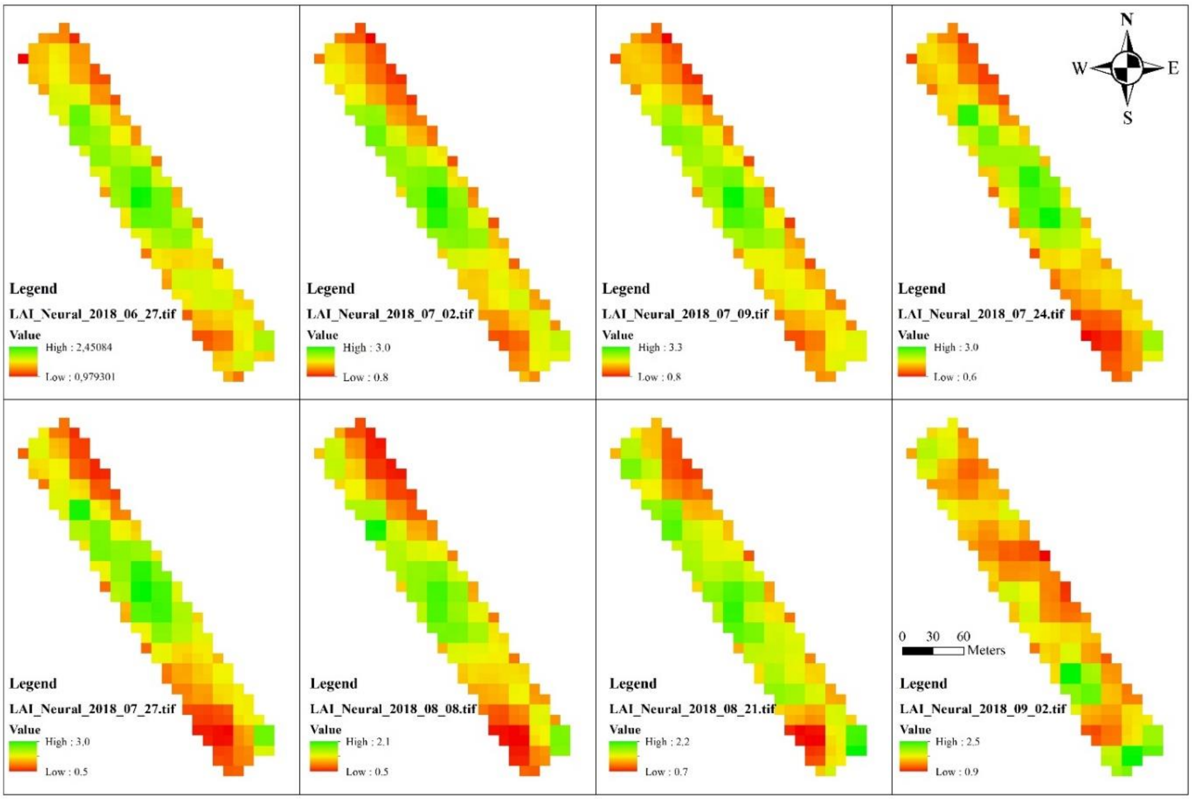

Figure 7. The spatial and temporal distribution of LAI estimated by neural network model

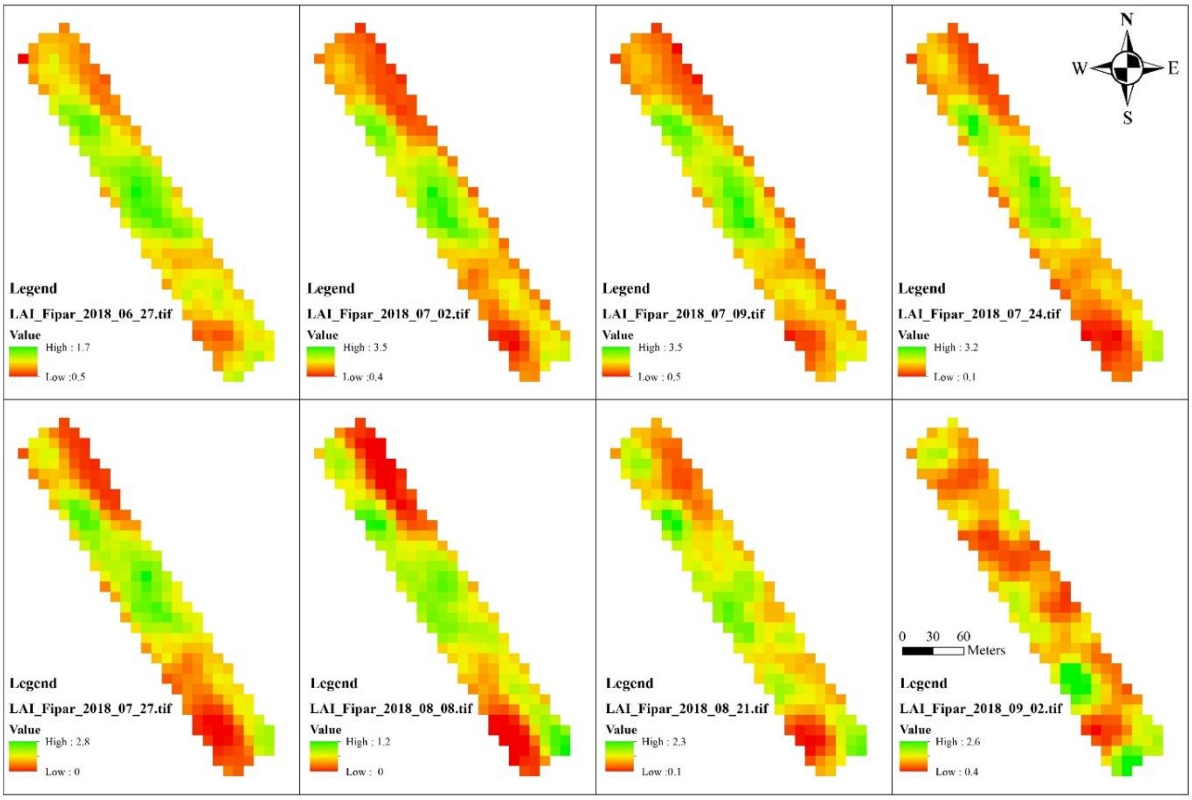

Figure 8. The spatial and temporal distribution of LAI estimated by Fipar calculation

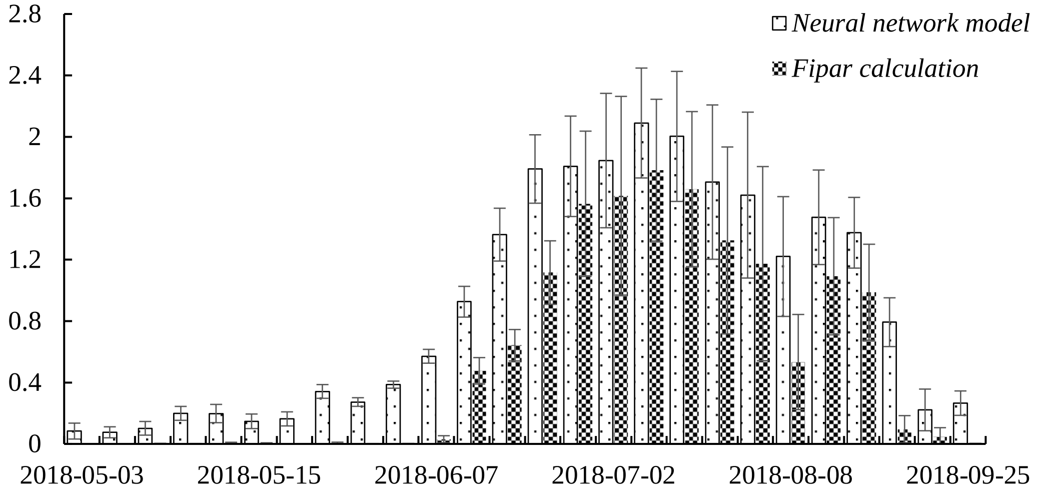

Figure 9.The temporal variation of average daily LAI estimated with two different methods.

Comparison of LAI estimated by two method.

The 22-days of data were used to compare the LAI values estimated using the two different methods.

Fig. 10 reveal that the LAI values estimated by the neural network model were generally higher than the LAI values estimated by the Fipar algorithm. Nevertheless, the linear fitting model as well showed that they were highly significantly correlated (R^2=0.89, p<0.01).

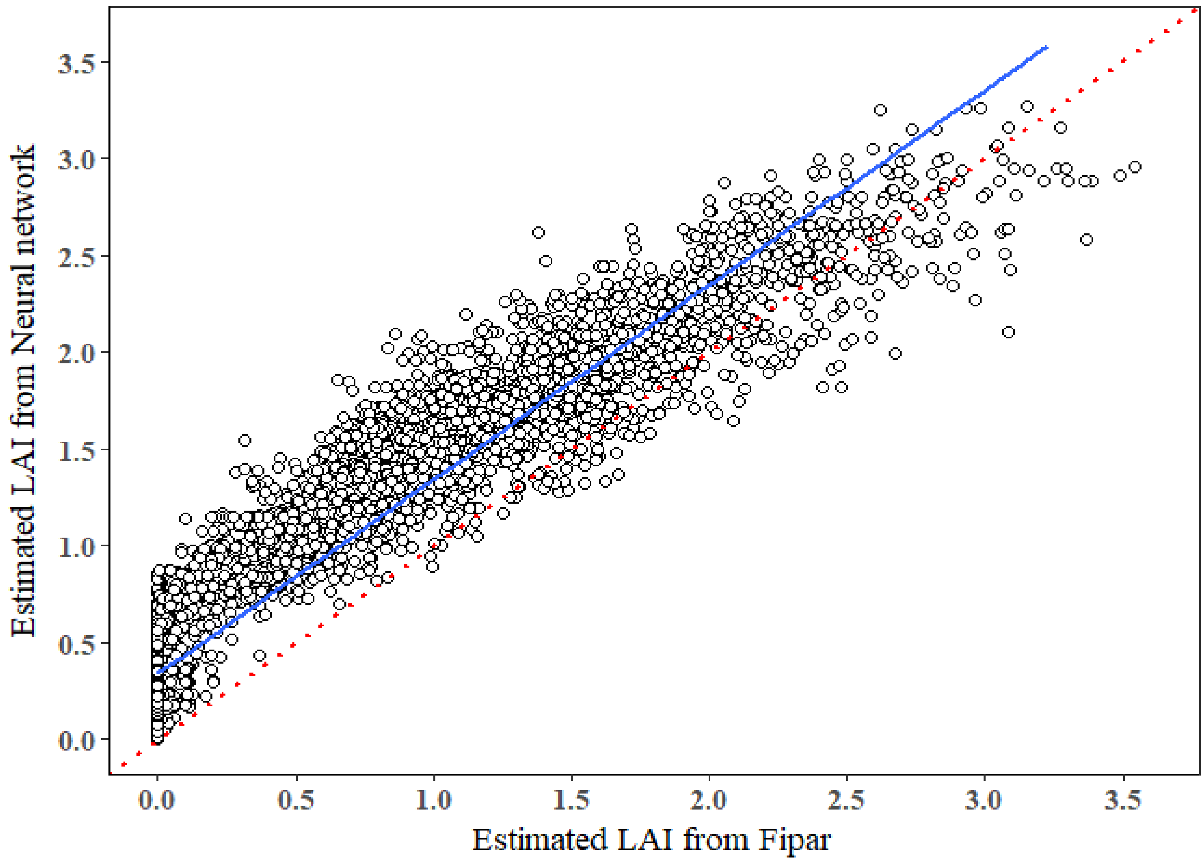

Figure 10. Comparison of the LAI estimated from two different methods. The stippled line in the plot is the 1:1 line. The R^2 value of the linear fitting model is 0.89 (p<0.001)

Discussion

Validation of the satellite reflectance and LAI derived from satellite

For the satellite image reflectance, the average value and standard deviation were similar to the ground measured reflectance. However, according to Fig. 4, the reflectance values fluctuated with a pattern that depended on the band and the magnitude of the reflectance. In general, due to the lower spatial resolution (10 x 10 meters), the fluctuation of the satellite data would be expected tobe smaller than rapidscan. It is therefore interesting that the fluctuation of the values from the satellites' near infra-red reflectance varied more than those fromrapidscan. A possible reason may be that in the field, plant growth in the individual plots varied very much between rows and since the rapidscan measurements were done in the same row every time, they may not be representative for the plot as a whole. However, this theory fails to explain why rapidscan data are always higher than satellite in low and lower than satellite data at high near infrared reflectance. This points to a more fundamental problem of mismatch in sensitivity between satellite and rapidscan instrument.. From figure 5, we can found that the relationship of the near infrared and red reflectance measured from satellite and rapidscan. The linear fitting model gave the same R square value, 0.54, which means the band will not affect the relationship of them.

Comparison of the two different LAI estimation methods

From Fig. 10, it is obvious that the LAI estimated from the neural network training model fitted well with the LAI estimated from the Fipar calculation. The only problem was that the values derivedwith the neural network-training model was higher than the values from Fipar calculation. The reason is likely that the LAI setting of the neural network-training model, 0-15, is much higher than the normal LAI in the field (Table 1). The range, 0-15, is for the whole globe scale LAI calculation. So it did not fit the local special situation, and the solotuion would be to lower the setting of this value. This was also the reason why in May, there were still some LAI with positive value calculated from the neural network model (the LAI should be almost zero that time since the potato field was bare soil during May). Therefore in Fig. 10, there were many zero values for LAI from Fipar calculation, which seems more reasonable.

Conclusion

In this research, two different LAI estimation methods were tried to estimate LAI. The ground measurement data of the reflectance based on rapidscan and LAI by LAI-2000 was used to validate the data. The result showed that the reflectance values from satellite and rapidscan did not follow the same pattern (R^2, 0.54), and the LAI estimated using the two methods did not fit well with the ground measurements of LAI. Possible reason should be that the satellite data is more coarse and it needs more ground measurement data to compare with it. However, the LAI estimated using the two different methods fitted well. This indicate that both of the models can be used to measure LAI after validation. Even though the LAI estimated from neural network model was higher than the LAI estimated form Fipar calculation method, it can be solved if the the input parameter are adjusted to reflect the maximum LAI expected for a given crop and place.Finally, it should be noted that LAI-2000 estimates of LAI, while usually quite precise, are prone to error when measuring in potato, due to the non-homegeneous canopy (rows). And as well the precondition of good measurement, that there has to be certain distance between sensor head and nearest leaf, probably often is violated.

Acknowledgement
The author would like to express great appreciation to Researcher, Héctor Nieto, and technician, Jofre, Christian in Efficient Use of Water program IRTA Spain. Thanks for their helpful advice about the calculation method and data processing.

References

Andersen, M.N., Heidmann, T. and Plauborg, F., 1996. The Effects of Drought and Nitrogen on Light Interception, Growth and Yield of Winter Oilseed Rape. Acta Agriculturae Scandinavica, Section B — Soil & Plant Science, 46(1): 55-67.

Asrar, G., Fuchs, M., Kanemasu, E.T. and Hatfield, J.L., 1984. Estimating Absorbed Photosynthetic Radiation and Leaf Area Index from Spectral Reflectance in Wheat1. Agronomy Journal, 76(2): 300-306.

Bacour, C., Baret, F., Béal, D., Weiss, M. and Pavageau, K., 2006. Neural network estimation of LAI, fAPAR, fCover and LAI×Cab, from top of canopy MERIS reflectance data: Principles and validation. Remote Sensing of Environment, 105(4): 313-325.

Breda, N.J., 2003. Ground-based measurements of leaf area index: a review of methods, instruments and current controversies. Journal of experimental botany, 54(392): 2403-17.

Campbell, G.S., 1977. An introduction to environmental biophysics / Gaylon S. Campbell. Heidelberg science library. Springer-Verlag, New York.

Campbell, G.S. and Norman, J.M., 1998. An Introduction to Environmental Biophysics. Springer, 104 pp.

Chen, J.M. and Cihlar, J., 1996. Retrieving leaf area index of boreal conifer forests using Landsat TM images. Remote Sensing of Environment, 55(2): 153-162.

Chen, J.M. et al., 2002. Derivation and validation of Canada-wide coarse-resolution leaf area index maps using high-resolution satellite imagery and ground measurements. Remote Sensing of Environment, 80(1): 165-184.

Christensen, S. and Goudriaan, J., 1993. Deriving light interception and biomass from spectral reflectance ratio. Remote Sensing of Environment, 43(1): 87-95.

Colombo, R., Bellingeri, D., Fasolini, D. and Marino, C.M., 2003. Retrieval of leaf area index in different vegetation types using high resolution satellite data. Remote Sensing of Environment, 86(1): 120-131.

Jacquemoud, S. and Baret, F., 1990. PROSPECT: A model of leaf optical properties spectra. Remote Sensing of Environment, 34(2): 75-91.

Kimes, D.S., Knyazikhin, Y., Privette, J.L., Abuelgasim, A.A. and Gao, F., 2000. Inversion methods for physically-based models. Remote Sensing Reviews, 18(2-4): 381-439.

Malouf, R. and Groningen, R., 2009. A Comparison of Algorithms for Maximum Entropy Parameter Estimation, Coling-02 : Proceedings of the Conference on Natural Language Learning, pp. 49-55.

Manevski, K., Lærke, P.E., Jiao, X., Santhome, S. and Jørgensen, U., 2017. Biomass productivity and radiation utilisation of innovative cropping systems for biorefinery. Agricultural and Forest Meteorology, 233: 250-264.

Marie Weiss, F.B., 2016. S2ToolBox Level 2 products: LAI, FAPAR, FCOVER.

Monteith, J.L. and Ross, J., 1981. The radiation regime and architecture of plant stands. Springer Netherlands, 344 pp.

Ramírez-García, J., Almendros, P. and Quemada, M., 2012. Ground cover and leaf area index relationship in a grass, legume and crucifer crop, 58, 385-390 pp.

Verhoef, W., 1985. Earth observation modeling based on layer scattering matrices. Remote Sensing of Environment, 17(2): 165-178.

Watson, D.J., 1947. Comparative Physiological Studies on the Growth of Field Crops: I. Variation in Net Assimilation Rate and Leaf Area between Species and Varieties, and within and between Years. Annals of Botany, 11(41): 41-76.

Zhou, Z., Plauborg, F., Thomsen, A.G. and Andersen, M.N., 2017. A RVI/LAI-reference curve to detect N stress and guide N fertigation using combined information from spectral reflectance and leaf area measurements in potato. European Journal of Agronomy, 87: 1-7.

New crop models including catch crops

Katarzyna Dorota Gielnik

Introduction

Leaf Area Index (LAI) is an an important measure for both theoretical and practical agriculture. It can be estimated from the ratio of red to infra-red light reflected from the field (see previous chapter of the report), but even that requires going to the field to measure it. However, for a given species, it has a relatively stable trajectory following the cumulative temperature sum. This is the approach that has been used for forecasting LAI in the Vandregnskab model, where it's used to predict when fields need irigation. In order for new species to be included in Vandregnskab, we need to:

a) Establish that the given species is stable in its relationship between temperature sum and LAI

b) Estimate the temperature sum demands for that species and the relationship between temperature sum and LAI, switch between growth phases (linear, exponential, flatline, decline), and

c) Estimate the growth parameters for the growth phases applicable to the species.

Data and calculations

Data were made available from the period 2015-2017 AU-Foulum resources, project monitoring the growth of catch crops. Likewise, we obtained daily temperature sums measured from the Foulum weather station in the corresponding period.

For all crops planted in spring, we used the data from the date of emergence, estimated as 10 days later than the date of planting, until harvest time. In this data set, the catch crops or undersown crops were all planted before the harvest of the maincrop, so instead of the planting date, their growth periods started the day after harvest of the maincrop (or any previous harvest, in the case of grass-clover, which had three harvests per year).

Data from the year 2017 was excluded because of suspicions of a spreadsheet error. Across every Maincrop, Subcrop, and PlotKey, the RVI measures are exactly equal for the dates 2017-05-31 and 2017-06-08. As seen below, this shows up as exactly parallel lines in the plot (right column). There is no room for doubt that this data was somehow copied or entered twice with different dates, but with the information available, there is no way of knowing which of the two dates is the correct date for those measurements.

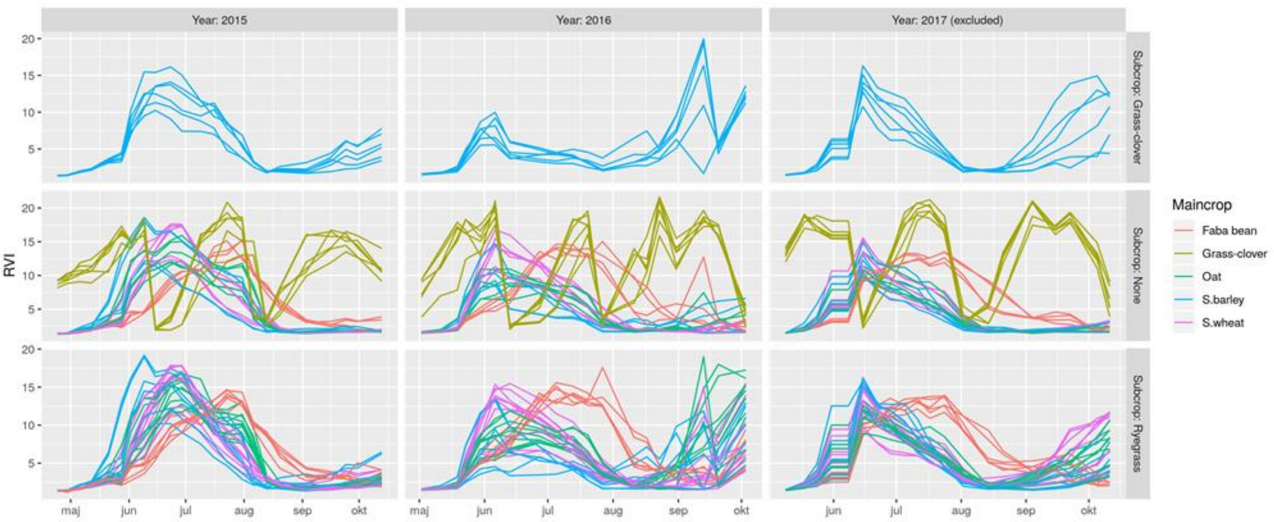

To estimate LAI from the ratio of red to infrared reflectance (RVI), the established practice was followed, to link it via the fraction of photosyntetically active radiation captured. This was done in R (see attached code) according to procedures previously implemented in MS Excel (provided by Mathias as a template).
For validation purposes, we had some data available from one field where both RVI and LAI were measured directly. The estimated LAI was correlated with the measured LAI with r = 0.66. Similar results were achieved using both equations to estimate LAI from fpar:

- LAI = log(1 - fpar) / -0.7
- LAI = log(1 – fpar) * -2 * cos(angle of sun at zenith)

This was only a moderate correlation, but it is also based on little data.

Results and discussion

In the following plots, each coloured line represents one plot in one harvest season. All of the maincrops in this data set showed enough similarities in their growth trajectories that we could move on with estimating them. The black lines with the main crops are the averages in each growth phase, according MARKVAND's growth model. However, it doesn't seem possible to blindly apply the same model to the subcrops studied here (see plots below).

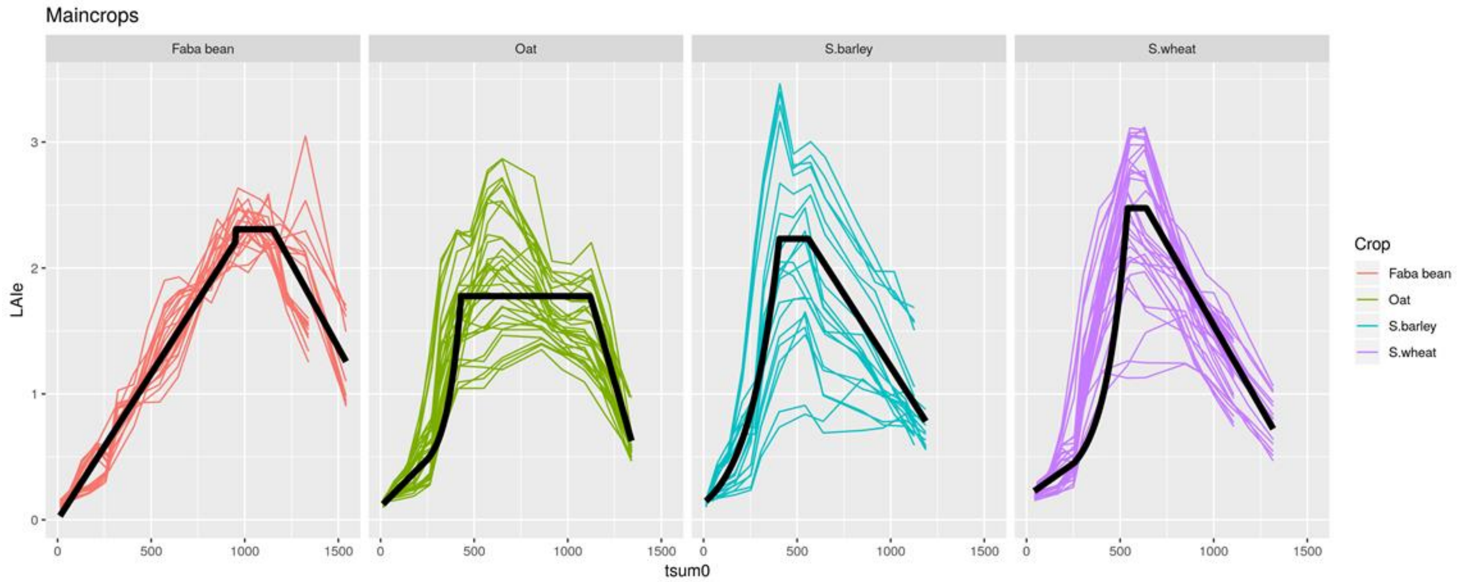

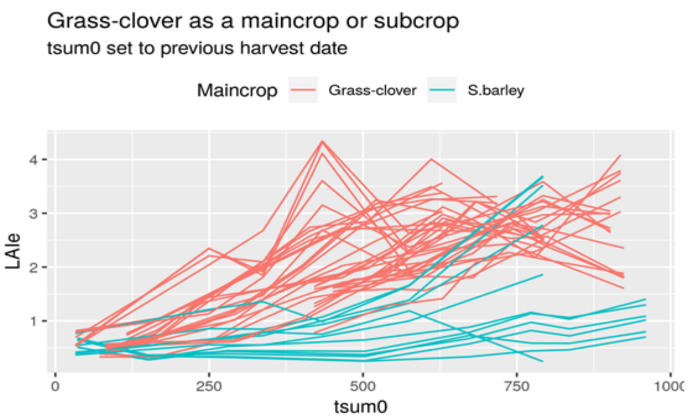

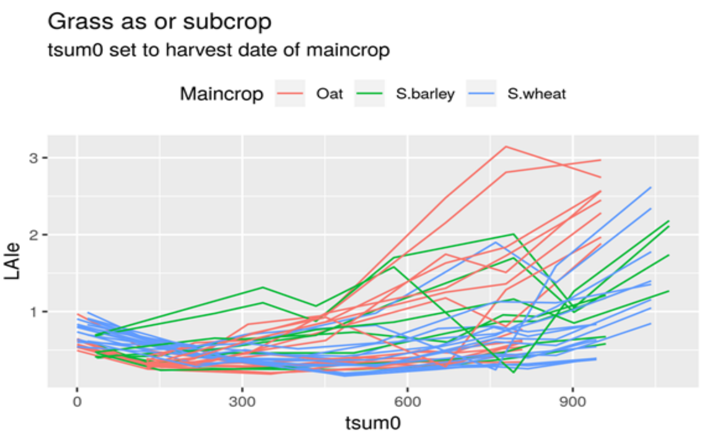

In the next step, the estimated leaf areas were fitted to the model for leaf areas' depence on temperature sums as described in Vandregnskab (Plauborg and Olesen, 1991). Once properly labelled, using the temperature sum since the date of emergence, the changepoints between the linear, exponential, flat, and declining growth phases were easy to see by eye on the graph above for maincrops. In general it can be a hard problem to get right, needing complex modelling strategies, but given the granularity in this data set, as well as the fact that we only had data from two different years, it would be hard to get much better estimates, even with a sofisticated modelling strategy. In particular, the precise values shown here are very dependent on the particular dates the data was sampled on.

Crop	**Sle**	**Slx**	**Slr**	**Slm**
Spring barley	0	405	560	1157
Spring wheat	255	540	640	1212
Oat	250	430	1120	1336
Faba bean	950	950	1150	1441

Given the temperature sum demands above, the problem can now be simplified to a series of ordinary regressions. A line was fitted to the linear growth phase and estimated Lgv and Lge as the average LAI predicted at the start and end of the linear growth phase, respectively. Lgx was chosen as the average LAI during the flat phase, and Lgm as the average LAI predicted at the end of a linear model fitted to the decline phase

Crop	**Lgv**	**Lge**	**Lgx**	**Lgm**
Spring barley	0.132	0.132	2.23	0.782
Spring wheat	0.185	0.452	2.48	0.722
Oat	0.104	0.480	1.78	0.626
Faba bean	0	2.21	2.31	1.26

Following the above calculation scheme, which has been developed partly as an application in R, we will derive a parameterization for Vandregnskab for the different catch crops included in the dataset and additional data measured in SEGES field experiments in 2018.

References

Plauborg, F. & Olesen, J.E. 1991. Udvikling og validering af modellen MARKVAND til vandingsstyring i landbruget. Tidsskr. Planteavl Beretning S-2113, 103 pp.

Maximal effective rooting depths and root zone capacity maps

Emmanuel Arthur, Mogens H. Greve, Mette Greve, Mathias Neumann Andersen
Department of Agroecology, Aarhus University, Blichers Allé 20, 8830 Tjele, Denmark

Introduction

Root zone capacity (RZC) may be described as the volume of water per unit of area within reach of plant roots for transpiration. Thus RZC is determined both by the extent of the roots of the crop in question as well as the properties of the soil it is grown in. The RZC controls the available water in the root zone and consequently determines the type and extent of vegetation (Tang et al., 2015). Discharge and soil water storage are two other processes that are strongly influenced by RZC. Despite its obvious importance, accurate estimates of RZC (that considers crop type, soil type and climatic variables) are not easily found in literature. This may be due to the lack of soil and plant root observations for large enough areas that can allow extrapolation to the field or catchment scale (Zhao et al., 2016). Important variables to consider in the estimation of RZC are the crop type and the environmental conditions. The strong influence of crop type on RZC primarily arises from the different rooting systems (density and length) of different crops. Some studies also point out that root depth is strongly related to climate (precipitation and potential evapotranspiration), providing data that show that climate-derived RZC estimates were more accurate than soil-derived RZC estimates for natural catchments (de Boer-Euser et al., 2016). Some estimation models also assume that crops that have the same vegetation functional type will have the same rooting depth, ignoring the environmental adjustments (Wang-Erlandsen et al., 2004). Other modeling techniques predict the rooting depth based on soil, climate and vegetation information (Collins and Bras, 2007). Although this approach is the ideal one, the use of such techniques is constrained by the unavailability of such data in several regions. It is therefore important to be able to consider both crop type and the soil type in any estimation method for RZC. This section focuses on revision of the current RZC estimation methodology in the Vandregnskab software by proposing new equations for estimation of PAW and revise rooting depth categorization based on soil type and crop type.

Data and calculations

Revision of estimation of PAW

In the current version of the Vandregnskab program, different values have been used over the years for the maximum effective rooting depth and root zone capacity of different soil types. The estimation of plant available water (PAW) in the program is based on the following equation:

$$\mathrm{PAW(Vol\%)} = (1.79\times\mathrm{OM}) + (0.07\times\mathrm{clay}) + (0.29\times\mathrm{fine\ silt}) + (0.18\times\mathrm{fine\ sand}) + 2.56 \qquad (1)$$

where clay, fine sand and fine silt, are respectively, <2 µm, 2-20 µm, and 20-200µm. We propose update to Equation (1) based on a more comprehensive dataset from Sunberg et al. (1999):

$$\mathrm{PAW(Vol\%)} = (1.96\times\mathrm{OM}) + (0.02\times\mathrm{clay}) + (0.34\times\mathrm{fine\ silt}) + (0.17\times\mathrm{fine\ sand}) + 2.26 \qquad (2)$$

Results and discussion

Effective rooting depth based on soil texture and organic matter:

Root depths were calculated based on the following scenarios for the soil properties and assigned to one of five categories (Table 1). For each category, the organic matter or humus (OM) and clay contents and in some cases the pH are used to identify the average rooting depth.

Table 1. Categories of rooting depth based on soil clay content and organic matter or humus

Category	Rooting depth (cm)	Soil conditions/scenarios
1	30	- (OM × 3 + clay) <= 6% in 0 – 60 cm depth
2	40	- (OM × 3 + clay) > 6% in 0 – 30 cm depth, *and* (OM × 3 + clay) <= 6% in 30 – 60 cm depth

3	70	- (OM × 3 + clay) > 6% in 30 – 60 cm depth, *and* (OM × 3 + clay) <= 6% in 60 – 100 cm depth
4	110	- (OM × 3 + clay) > 6% in 30 – 100 cm depth, *and* (OM × 3 + clay) <= 6% in 100 – 200 cm depth - (OM × 3 + clay) > 6% in 30 – 200 cm depth *and* pH <= 5.6 in 100 – 200 cm depth
5	150	- (OM × 3 + clay) > 6% in 30 – 200 cm depth *and* pH > 5.6 in 100 – 200 cm depth

The eventual RZC is calculated as a weighted sum down to the rooting depth, and the maximum value possible is:

$$A\ \mathrm{PAW}\times 3 + B\ \mathrm{PAW}\times 3 + C\ \mathrm{PAW}\times 4 + D\ \mathrm{PAW}\times 5 \qquad (3)$$

with A, B, C, and D being depths of 0 – 30 cm, 30 – 60 cm, 60 – 100 cm, and 100 – 200 cm, respectively.

Based on the revised PAW estimation from Equation (2), the crops can be grouped into three categories based on the estimated maximum rooting depth. The maxium rooting depth categories were made based on the previous estimates built in Vandregnskab and the current literature (e.g., Fan et al, 2016 and references therein associated with Table 1 in their paper)

Table 2. Maximum root depth categories for crops

Category	Depth, cm (range)	Examples of crops
1	70 (50-80)	Potatoes, peas,
2	90 (80-110)	maize, spring barley, spring rape, sugar beet, winter wheat, barley, rape and rye
3	130 (110-140)	Alfalfa, ryegrass,

Thus, based on the revised soil texture and organic carbon maps (example shown for the A horizon below in Figure 1) and the crops that are grown on each field, the RZC can be estimated for the entire country.

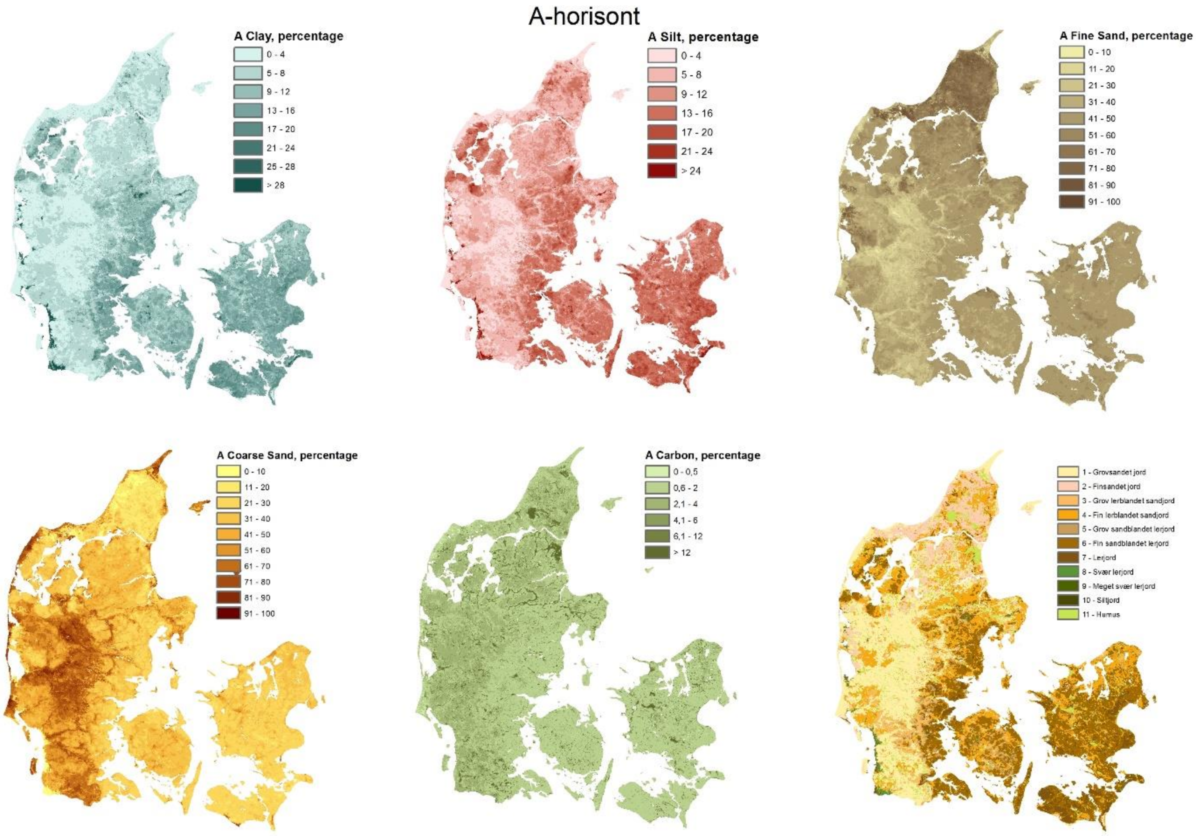

Figure 1. Soil particle size distribution and organic carbon of the A horizons in Denmark.

An example of the estimated RZC map for medium-rooted crops (category 2 in Table 2) is shown below in Figure 2:

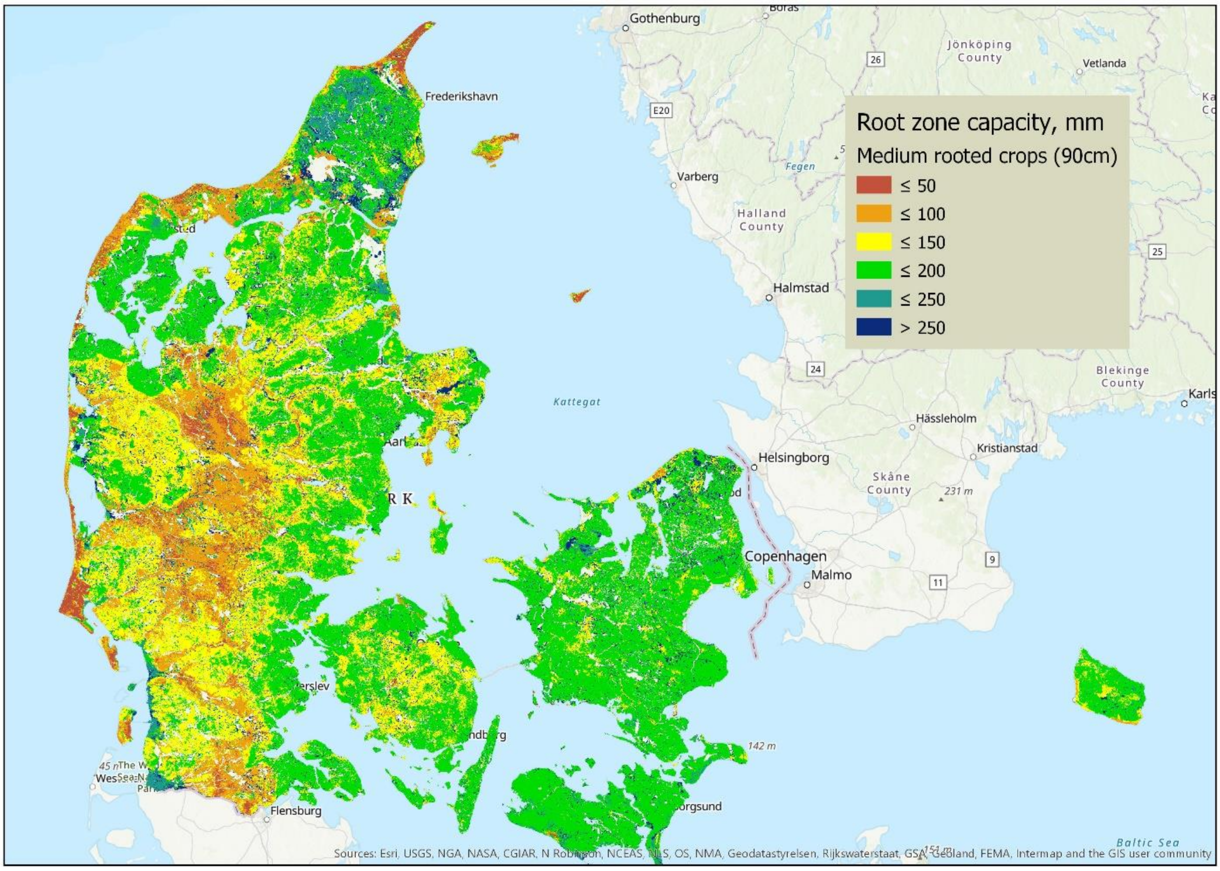

Figure 2. Root zone capacity distribution for medium-rooted crops

Based on the above, the application of this revision of rooting depth and RZC requires knowledge of the soil horizonation, the soil clay content, organic matter and soil pH. Based on Equations 2 and 3, and Tables 1 and 2, the RZC can be estimated for all types of crops and soil types

References

Tang, G., Carroll, R. W., Lutz, A., & Sun, L. (2016). Regulation of precipitation-associated vegetation dynamics on catchment water balance in a semiarid and arid mountainous watershed. *Ecohydrology*, *9*(7), 1248-1262.
Zhao, J., Xu, Z., & Singh, V. P. (2016). Estimation of root zone storage capacity at the catchment scale using improved Mass Curve Technique. *Journal of Hydrology*, *540*, 959-972.
de Boer-Euser, T., McMillan, H. K., Hrachowitz, M., Winsemius, H. C., & Savenije, H. H. (2016). Influence of soil and climate on root zone storage capacity. *Water Resources Research*, *52*(3), 2009-2024.
Wang-Erlandsson, L., Van Der Ent, R. J., Gordon, L. J., & Savenije, H. H. G. (2014). Contrasting roles of interception and transpiration in the hydrological cycle–Part 1: Temporal characteristics over land. *Earth System Dynamics*, *5*(2), 441-469.
Collins, D. B. G., & Bras, R. L. (2007). Plant rooting strategies in water-limited ecosystems. *Water Resources* Research, 43(6).
Sundberg, P.S (red.), Callesen, I, Greve, M. H., & Raulund.Rasmussen, K. (1999). Danske jordbundsprofiler. Danmarks JordbrugsForskning, Foulum.
Fan, J., McConkey, B., Wang, H., & Janzen, H. (2016). Root distribution by depth for temperate agricultural crops. *Field Crops Research*, *189*, 68-74.

Models for calculating yield loss due to drought

Mathias Neumann Andersen

Introduction

Careful planning and scheduling of irrigation are perhaps more important today than ever before, where the farmer is left with a marginal return on investments in labour, seeds, fertilizers, etc due to the decreasing market prices on most agricultural crops. It is not at all an easy task to manage irrigation in a rotation of several crops, as prevalent on most Danish farms, and harvesting of the expected returns can only be realized by successful decisions during the season. Likewise, the impact of irrigation on the environment has to be considered. Water consumption and nitrogen leaching can both be effectively reduced by intelligent application of irrigation water.

Any discussion of critical drought stresses in crops and approaches to avoid them should be based upon a sound knowledge of water transport in the soil-plant-atmosphere system. To this end the results of a vast number of scientific investigations, on levels ranging from subcellular to whole catchments with several crops, are available in literature. Since by nature farming requires as well economical as several technical skills, no one can expect the farmer to overview the whole body of this knowledge on crop response to irrigation. However, the use of personal computers and model calculations have given the opportunity to comprehend the results of research in computer systems, which can aid decisions.

Hiler and Howell (1983) stated three areas that "offer considerable promise towards increased efficiency of water use:

Improved irrigation scheduling techniques, (ii) improved irrigation water application and distribution systems, and (iii) application of system optimization methods to improve the on-farm water allocation to crops.

Translated to the conditions of Danish farm units this means that a computer system must have the following features: (i) Irrigation amounts to the individual fields have to be calculated precisely. Since irrigation capacity is limited and the work has to be planned, the system must be able to predict irrigation demands 3 to 5 days ahead by taking into consideration the meteorological forecasts. Furthermore the system has to be user-friendly, easy to understand and operate using a minimum of time. (ii) Apply to current irrigation systems, which in the Danish context largely are dominated by raingun systems driven by electrical ground water pumps, although, older sprinkler and newer center-pivot systems can be found. (iii) Last but not least the economical return of the total farm effort must be optimized.

Based on these considerations a water balance model Vandregnskab for on-farm irrigation scheduling was developed (Plauborg & Olesen, 1991; Thysen & Detlefsen, 2007) in close cooperation with the extension service, who tested and improved the user-interface. This article describes the development of a crop priority model to cover the third area i.e. to improve the on-farm water allocation to crops. Clearly, this allocation has to be based on the yield and quality response of agricultural crops to irrigation. If these are known the crops can be ranked according to which are the most profitable to irrigate in situations where the irrigation capacity is inadequate or situations where the profitability is questionable. To answer these questions experiments have been conducted to assess the yield and quality response to irrigation of a range of crops important to Danish agriculture. These experiments have also given information on the growth and crop area

index crucial for validation of the water balance model in Vandregnskab. Further, the work has comprised collection of data on yield and quality from former Danish irrigation experiments. Both new and old data were analyzed statistically to find the best possible description, in the form of crop-water production functions, of the relation between irrigation and yield and quality.
Finally, the relations were implemented in Vandregnskab as a superstructure to the water balance model.

Materials and methods

Experimental site

The irrigation experiments that were used in the analysis were conducted at Jyndevad Research Station in South Jutland. The soil at Jyndevad is a coarse-textured meltwater sand which contains c. 76 % coarse sand (0.2-2.0 mm), 15 % fine sand (0.02-0.2 mm), 4 % silt (0.002-0.02 mm) and 3 % clay (< 0.002 mm). In the top layer (0-20 cm) the organic matter content is about 3 % (Hansen, 1976). The soil is classified as an Orthic Haplohumod (Nielsen & Møberg, 1985) with a plant available water capacity of only c. 65 mm to a depth of 60 cm (Hansen, 1976), which is the maximum rooting depth for most agricultural crops on this soil type (Andersen, 1986; Andersen & Aremu; 1991, Andersen et al., 1992). The dry bulk density is about 1.55 g/cm3 for both the plough layer and the subsoil (Hansen et al., 1986). The average yearly precipitation at Jyndevad (1961-1990) was around 900 mm, which is relatively high compared to other places in Denmark.

Experimental design

At Jyndevad, irrigation experiments has been carried out since 1939 with many crops. The experiments were conducted both in the field and in sheltered facilities with an automatic roof covering the plots during rainfall events. Both in the field and in the sheltered experiments, irrigation water was usually applied through a trickle irrigation system with the irrigation lines mounted on a manually moveable aluminum frame above the crop and with the nozzles spaced in a 20 times 20 cm grid. For the irrigation of maize however, the lines were placed on the ground. The amounts of irrigation water were measured with flow sensors accurate to 0.1 l. A common experimental design was to divide the growing season into three periods depending on the crop's phenological stages: Vegetative, flowering and yield formation and then carry out treatments, which had one or more drying levels in each growth stage to a predefined soil water deficit. Most experiments as well comprised a fully irrigated treatment, that throughout the season was irrigated before 50% of the available water in the roozone was used up, as well as a treatment that was left unirrigated for the whole season. It has to be remembered that drought treatments under field conditions are always depending on the seasons weather conditions. It was not always possible to obtain the planned soil water deficits in the treatments.

Measurements

The environmental variables that were measured and used in analyses of crop growth comprised basic climatic and soil water data obtained from the meterological station (DMI) at Jyndevad. The climatic elements: global radiation, net radiation, relative air humidity, air and soil temperature, precipitation, wind speed, wind direction and soil heat flux were measured every 10 minutes. The experimental fields were situated mostly within a distance of less than 1 km from the meteorological station. In the experiments all plots were usually equipped with neutron access tubes or since the 90'ties with TDR (Time Domain Reflectometry, and soil water content was measured approximately weekly in the fully irrigated treatment (1), in the other treatments measurements were done once or twice a week during the respective drought periods. The neutron equipment has earlier been calibrated to establish a relation between neutron count per minute and gravimetric water content for 10 cm soil layers to a depth of 90 cm both in the field and in the shelter facility (Andersen & Thomsen, 1994). Usually plots were further equipped with tensiometers at 20 and 40 cm depth. These were read one or two times a week mainly to determine when a soil water deficit of 30 mm had been reached. At this level irrigation was applied in the fully irrigated treatment and in the other treatments outside the growth stages where drought periods had been planned. Like for the neutron equipment a relation had been established between tensiometer readings and soil water deficit in the 0 - 60 cm depth. For the TDR probes as well a site specific calibration was available (Jacobsen & Schjønning, 1993a,b).

Crop and plant response to the treatments and the environment were characterized from measurements of phenological development, growth of shoot and roots, chemical composition of dry matter, canopy spectral reflectance, light interception, plant water relations and leaf photosyn-thesis. Since some of these methods are rather time consuming a top down approach had to be selected to ensure that basic growth and yield data needed for the development of the Vandregnskab model became available for all crops, while physiological causes for the observed plant responses were investigated mainly in one crop: winter oilseed rape.

Phenological development was assessed weekly according to growth stage keys for the individual crops and at the same time crop height was measured. Samples for growth analyses were taken in the field experiments. Four small areas of 0.5040 m2 for most crops and 1.5692 m2 for beets and potatoes were marked in the spring in each plot. Samples for growth analyses were taken with approximately 10 days intervals in treatments that were fully irrigated until the time of cutting and additional 2-3 samples were taken in drought stressed treatments during and after drought. The samples were obtained by cutting of the shoots at the soil surface or for beets by collecting the whole plants including the storage root. The samples were sealed in plastic bags and brought to nearby laboratory for analysis. In the laboratory total fresh weight and dry matter percentage of the shoots and roots were measured. A subsample of about one third of the shoot material was further analyzed by separating it into green and yellow leaves, green and yellow stems and green and yellow ears or siliques. The one-sided surface area of the green fractions were measured by a leaf area meter (Li-cor model 3050A; Li-cor Inc., Lincoln, NE, USA). The dry weight of all fractions were then determined to enable calculation of crop area indices based on the ratio between the dry weight of the whole and the subsample. Dry weights were obtained by drying the material at 80^o C for 16-24 hours in a ventilated oven. On the last sampling date before harvest the number of plants and ears or siliques in the subsample were counted to enable calculations of yield components. The dried material from the analysis of dry matter percentage was sent to the Central Laboratory of the Min-istry of Agriculture for determination of the concentrations of N, P, K, Ca and Mg. N was determined by the Kjeldahl procedure while cations and P were extracted from ashed tissue (450^o C, 4 h) with dilute HCl/HNO3. Ca and Mg were measured by atomic absorption spectrometry, K by flame photometry and P by spectrophotometry after complexing with vanadium. In a few crops, soil samples were taken for determination of rooting depth. Root length was determined by the line intersect method (Newman, 1966) modified to obtain at least 100 intersects per sample, thereby reducing the error caused by the counting procedure. The fresh and the dry weight of the roots were finally measured and concentration of N, P, K, Ca and Mg determined as for the shoot material.

At harvest time crops from the field experiments were harvested directly by a combiner with the same width as the plots (width: 2.40, length: 3.40 m). Both seeds and straw from each plot were taken to the laboratory to be weighed and to determine the dry matter percentage. Finally, from each plot 0.5040 m2 of the stubble was removed and the dry weight determined. Fodder beets were taken up by hand and separated in storage root and leaves. Seed weight in each plot was determined by weighing of 200 seeds dried at 80^o C for 16-24 hours. Seeds and straw was analyzed for the concentrations of N, P, K, Ca and Mg. Additionally, oil concentration of the oilseed rape seeds was determined by milling the seed in liquid nitrogen followed by extraction of the oil with diethylether for c. 16 hours. In silage maize 10 cobs per plot were separated in cover leaves, seeds and shank and the dry weight of 200 seeds determined. These fractions and the stalk were analyzed for the concentrations of N, P, K, Ca and Mg. Furthermore, to determine the feeding value for cattle, the concentration of in-vitro soluble organic matter was analyzed by fermenting samples in rumen fluid for 48 h followed by incubation with pepsin-HCl solution for another 48 h. Also, the concentration of crude fibre was determined after removal of proteins and carbohydrates from the samples with boiling, dilute sulphuric acid (0.13 M, 0.5 h) and potassium hydroxide solution (0.23 M, 0.5 h). Finally, oil concentration of the seed was determined. In beets the concentrations of N, P, K, Ca, Mg, in-vitro soluble organic matter and crude fibre were determined in the leaf and the storage root fractions.

From 1988 the spectral incoming and reflected radiation were measured to allow calculation of light interception of the crops. In the 1989-92 seasons an 8-band radiometer (model: CROPSCAN), was used. The sensors consisted of 8 or 4 pairs of silicon photodiodes equipped with specific interference filters transmitting wavelengths in intervals of 50 nm from 500 to 850 nm. One sensor of each pair was facing upwards recording incident radiation and the other downwards recording reflected radiation. The upward sensors were covered by a diffuser of flashed opal glass while the downward sensors had their angle of view restricted to 28 degrees by a convex 18 mm lens. The analog output from the sensors was passed through an A/D converter and collected by a small computer. The whole system was portable with the sensor head mounted on an aluminium arm of adjustable length. Due to deteriorating filters the equipment was substituted in 1993 with a similar radiometer (Skye Instruments, ND, USA) with only two pairs of sensors measuring incident and reflected radiation in a red band around 650 nm and a near infrared band around 800 nm. Measurements were taken approximately weekly in all plots. The sensor head was fixed at height of 2.0 m giving a circular field of view with a diameter of half the height i.e. 1.0 m. Additionally, spectral reflection of the areas used for the growth analyses was measured immediately before sampling the material with the sensor head positioned at 1.25 m height to measure reflection from small areas only. Measurements were taken between 10.00 h and 14.00 h without considering cloud cover but taking care to avoid shadows from the person who took the measurements. To relate the spectral reflection to the fractional interception of photosynthetically active radiation (fPAR) measurements were taken with a line quantum sensor (model LI-191¬SB, Li-cor Inc.) inserted at the soil surface below the crop and a quantum sensor (model LI-190SB, Li-cor Inc.) above the crop. Both sensors were connected to a datalogger (model LI-1000, Li-cor Inc.) to allow simultaneous measurements. In some cases the equipment was permanently installed in a plot measuring 10 minutes average values while in other years weekly instantaneous measurements were taken in all plots.

Statistical Analyses for parameterization of Crop Water Production Functions

To develop a crop priority model for the Vandregnskab-model covering a range of crop species we would like some resonable simple assessment of the effect of water deficit on final yield. So-called crop water production functions, which relate yield to some measure of (evapo-) transpiration seems to be appropriate in this connection since we want our estimates of drought sensitivity to be independent of soil type, location and year in the ideal case. Drought sensitivity estimates based on for instance soil water deficit clearly does not fulfil this. Furthermore, the water balance model in Vandregnskab already calculated daily transpiration but not physiological parameters as assimilate production or crop water potential.

de Wit (1958) showed that for dry, high-radiation climates, yield and transpiration were related as:

$$By/\Sigma Ta = m/E'p \qquad (1)$$

where By = biomass yield at harvest, ΣTa = sum of daily transpiration from emergence to harvest, and E'p = mean daily free water evaporation for the same period either calculated from pan data or the Penman combination formula. de Wit showed that the constant m was dependent mainly on species and “at first approximation” was independent of soil nutrition and water availability unless seriously nutrition-limited or soil water was in excess. The relation in Eq. (1) could be simplified for humid regions because when water was not limiting, fluctuations in radiation would not affect appreciably the ratio $\Sigma Ta/E'p$. de Wit found under these conditions that:

$$By/\Sigma Ta = n \qquad (2)$$

where n is a constant, gave a better description.

Bierhuizen & Slatyer (1965) later, on the basis of single leaf analyses, proposed that the two Eqs. (1) and (2) could be unified by taking into account the daily mean of the atmospheric water vapour pressure deficit (Δe) between sunrise and sunset:

$$By/\Sigma Ta = k/\Delta e \qquad (3)$$

A possible draw-back of the crop water production functions presented in Eqs. (1), (2) and (3) is that they are only valid when looking at the total biomass production. They do not take into account any variation in the respective m, n and k parameters, which can be present when looking at grain/seed yield related to the timing of drought stress or crop development. Especially for crops where only part of the total biomass yield is harvested and therefore of importance for the economic yield e.g. grain and seed crops, drought in particular growth stages may be critical for the harvested yield. Among a large number of yield versus transpiration relationsships (e.g. Vaux & Pruitt, 1983) we have chosen to develop the stress-day model of Mogensen (1980) to allow for a variation in drought sensitivity during the crop development:

$$(1 - Ya/Ym) = ky\ \Sigma(1-Ta/Tm) \qquad (4)$$

where Ya and Ta are the yield and the daily transpiration respectively of a drought stressed crop while Ym and Tm are the corresponding variables for a fully irrigated crop. ky is a drought sensitivity parameter which can be estimated when the other variables are known. This model includes the desirable feature for inclusion in a real-time model, that the relative yield decrease due to reduced relative transpiration can be evaluated on a daily basis provided that ky has been estimated previously.

To estimate ky, the number of stress-days ($Sd = \Sigma(1-Ta/Tm)$) can be summed for the entire season, individual growth phases with individual values of ky or the daily values can just be used with a continous variation of ky to allow for the timing of drought stress in relation to crop development. In the following we have chosen the last approach. Now consider a number of treatments with only one day of stress for which the drought sensitivity can be calculated from:

$$ky = (1 - Ya/Ym)/Sd \qquad (5)$$

then the calculated ky-values can be fitted to a polynomial-function of the temperaturesum (ts) from emergence or onset of growth (for winter crops):

$$ky = a + a1ts + a2ts2 + a3ts3 \qquad (6)$$

Since most treatments in our experiments contained more than one day of stress we expanded Eq. (5) substituting the expression for ky in Eq. (6) to describe the influence of multiple days of stress as:

$$(1 - Ya/Ym) = \sum_{i=1}^{n} Sdi(a+a1tsi+a2tsi2+a3tsi3) \quad (7)$$

where i is day-numbers between emergence and harvest. A similar multiplicative model reads:

$$Ya/Ym = \prod_{i=1}^{n} (1-Sdi(a+a1tsi+a2tsi2+a3tsi3)) \quad (8)$$

The parameters in Eq. (7) were estimated by the linear least-squares procedure REG of SAS (SAS Institute, 1988) and the parameters of Eq. (8) by the non-linear procedure NLIN.

Results and discussion

Development of Crop Water Production Functions

Since the data material comprises a large number of crops and years, we will not go into a detailed description of the entire background data. Instead, a few examples will be given to give the reader an impression of the calculation procedures that were pursued and finally the focus will be on the synthesis of results for all crops considered. An example of the accumulation of stressdays during a season as calculated by the MVTOOL software for unirrigated spring barley fields is shown in Fig. 1 for two years.

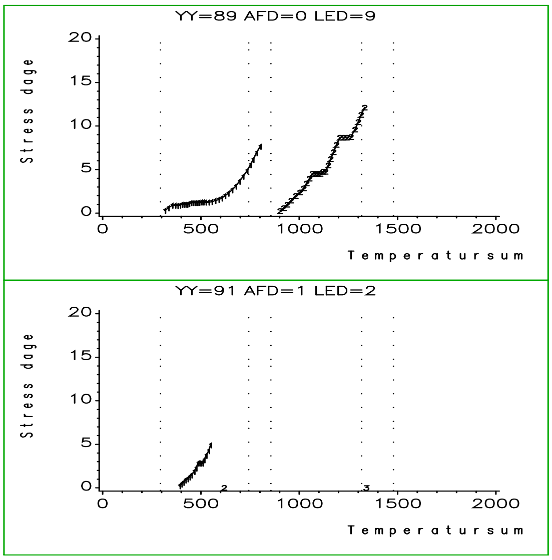

Fig. 1. Accumulated stressdays during drought periods in relation to development stage for unirrigated spring barley fields in 1989 and 91 at Jyndevad.

Phenological development and growth stages according to Vandregnskab are indicated by the temperature sum from emergence on the x-axis and growth stage changes shown by vertical dashed lines. From Fig. 1 it can be noted that in 1989 there was two rather long periods with drought in the vegetative stage and in the grain filiing stage of spring barley. 8 and 13 stressdays were accumulated, respectively. In 1991 there was only one short drought period during the beginning of the vegetative stage.

The case of winter oilseed rape

For winter oilseed rape a more thourough analysis was performed with the aim of looking behind the immediate effects of drought visualized in the form of the oil yield drought sensitivity functions.

DROUGHT SENSITIVITY OF OIL YIELD AND YIELD COMPONENTS OF WINTER OILSEED RAPE EXPRESSED AS A CONTINUOUS FUNCTION OF CROP DEVELOPMENT

Abstract

The water balance of eight irrigation experiments with winter oilseed rape conducted during 1982-1985 and 1991-1994 was simulated with the model MVTOOL and actual transpiration calculated. Because of a large variation in harvest index caused by drought, oil yield was not linearly related to aboveground biomass or cumulative transpiration. Instead, we developed a model based on daily relative transpiration deficit (stress-day) allowing for a continuously varying drought sensitivity, i.e. relative yield decrease per unit of stress-day, as a function of temperature sum. The curve for drought sensitivity changed from zero at the beginning of flowering to a maximum value of c. 8.6% at the middle of the flowering phase then had a second maximum of c. 8.4% at late pod-filling and went back to zero at the end of the pod-filling phase. A daily yield loss of 8.6%, which was higher than the potential production during one day, indicated that physiological reactions other than a reduced photosynthesis were causing the yield decrease under drought. Seed number and interception of photosynthetically active radiation during pod-filling had maxima of drought sensitivity corresponding in time and size to the two maxima for oil yield during flowering and pod-filling, respectively. Therefore, we conclude that abortion of pod and seed primordia during flowering and senescence of the pod canopy during pod-filling were the prime physiological processes leading to reduced yield of oil during drought. Also, the oil-concentration of seeds was reduced by drought while N-concentration was increased. The model developed is well suited for application in irrigation management systems built on water balance models.
Key words Brassica napus, Oil-concentration, Relative transpiration, Seed abortion, Senescence, Stress-day, Temperature sum

Introduction

Scheduling irrigation in order to obtain a maximum net economic return, necessitates the development of functions between economic yield of crops and water use. One example, for a wide range of crops, was given by Doorenbos & Kassam (1979). However, inherent to this approach are concerns about the generality of the functions, i.e. between different crops, climates, soils and the growth stages within a single crop. de Wit (1958) presented evidence that biomass production of a crop is proportional to transpiration in humid climates while for drier climates e.g. Tanner & Sinclair (1983) have argued that biomass production is proportional to daily transpiration divided by daily vapour pressure deficit.

During the season the crop was treated with pesticides to control weeds and insects. A gross plot size of 15.2 m2 was employed and irrigation water was applied through a trickle irrigation system with irrigation lines placed on moveable frames above the crop with drip nozzles spaced in a 20 by 20 cm grid. Irrigation water was measured with flow sensors accurate to 0.1 l. In the experiments the growing season was divided into the vegetative, flowering and pod-filling phase. Different levels of irrigation were applied in the phases as shown in Table 1. The treatment irrigated at 30 mm deficit (about half of the available water content) was considered to be fully irrigated. Over the eight years there were 50 treatments, but not all of the planned soil water deficits were achieved due to precipitation events. The plots were arranged in a randomized block design with 4 replications of each treatment.

Table 1. Irrigation treatments in winter oilseed rape. Irrigation levels were defined by the soil water deficit allowed to occur in the three growth phases p1: vegetative, p2: flowering and p3: pod filling.

Treat-ment	Irrigation at soil water deficit level (mm)		
	p1	p2	p3
1	30	30	30
2	40-50	30	30
3	30	40-50*	30
4	30	30	40-50*
5	unirrigated		

* In the 1991-1994 experiments there were more treatments with different deficit levels

During the season the crop was treated with pesticides to control weeds and insects. A gross plot size of 15.2 m2 was employed and irrigation water was applied through a trickle irrigation system with irrigation lines placed on moveable frames above the crop with drip nozzles spaced in a 20 by 20 cm grid. Irrigation water was measured with flow sensors accurate to 0.1 l. In the experiments the growing season was divided into the vegetative, flowering and pod-filling phase. Different levels of irrigation were applied in the phases as shown in Table 1. The treatment irrigated at 30 mm deficit (about half of the available water content) was considered to be fully irrigated. Over the eight years there were 50 treatments, but not all of the planned soil water deficits were achieved due to precipitation events. The plots were arranged in a randomized block design with 4 replications of each treatment.

Measurements

The climatic variables measured were global radiation, relative air humidity, air and soil temperature, precipitation, wind speed and wind direction. All elements were measured hourly at the local weather station with the experimental fields situated within a distance of 1 km. Plots were equipped with neutron access tubes or TDR-probes from 1993 and soil water content was measured weekly in the fully irrigated treatment (1), and once or twice a week in the remaining treatments during the respective drought periods. Two plots in each treatment were equipped with tensiometers at 22 and 40 cm depth. These were read once or twice weekly to determine when a soil water deficit of 30 mm had been reached. At this soil water deficit, irrigation was applied to the fully irrigated treatment and to the other treatments outside the drought periods.

Phenological development of the crops was assessed weekly according to the FAO growth stage key. The crop was swathed at the stage where about one-third of the seeds had turned brown and later harvested by combine. The seeds from each plot were taken to the laboratory to be weighed and to determine the dry matter percentage after drying at 80o C for 16-24 hours in a ventilated oven. Oil concentration of the seeds (O, weight-percent) was determined by milling seeds in liquid nitrogen followed by extrac-tion of the oil with diethylether for 16 hours. Yield of oil (Y, kg ha-1) was calculated from seed yield and oil concentration. In the 1991-1994 experiments, dry seed weight in each plot was also determined by weighing 200 seeds dried at 80o C for 16-24 hours and number of seeds per unit area (N, m-2) was derived from seed yield and seed weight. The amount of straw and stubble was determined so that total aboveground biomass at harvest was measured. Further, during the 1991-1994 seasons, weekly measurements of canopy spectral reflectance were taken from which interception of photosynthetically active radiation (PAR) by green crop parts (I, MJ m^{-2}) was calculated (Andersen et al., 1996).

Analyses

The water balance of each treatment was modelled with the MVTOOL model (Olesen & Plauborg, 1995). MVTOOL consists of empirical submodels for crop development and soil water balance, which are updated using daily time steps. The same submodels are used with a user interface in the MARKVAND irrigation scheduling system (Plauborg et al., 1996). Standard parameters for soil type and leaf area development were used together with daily evapotranspiration calculated from a modification of Penman's (Penman, 1956) formula developed by Mikkelsen & Olesen (1991) to simulate the water balance of each treatment. It was necessary to ensure accurate simulation of the water balance in order to develop crop-water production functions. Comparisons were made between neutron or TDR measurements of soil water deficit in the individual plots and the simulated values. For some of the treatments differen-ces were found which could be due to limitations in the model, errors in meteorological data, errors in measurements of soil water deficit or an unusual crop development. If the difference between simulated and measured deficits was large, the treatment was excluded from the analysis. Another test on the remaining experiments was performed, where the accumulated actual evapotranspiration simulated by MVTOOL was related to measured actual evapotranspiration in periods where drainage was unlikely to occur (Plauborg et al., 1996). Also the model describing leaf area development was tested by comparisons between simulated leaf area and light interception measured during 1991-1994. After these tests 45 treatments out of a total of 50 remained for further analysis.

The stress-day index (S_d) was defined as:

$$S_d = \left(1 - \frac{(E_{aT}+E_{aIg})}{E_{pT}}\right) \quad \mathbf{1}$$

where E_{aT}, E_{pT} are daily actual and potential transpiration (mm day^{-1}), respectively, and E_{aIg} is evaporation of intercepted water on green leaves (mm day^{-1}).

Relative oil yield in the treatments (Y_a/Y_m) and relative oil yield decrease ($1-Y_a/Y_m$) were calculated from measured actual yield of oil (Y_a, kg ha^{-1}) divided by the maximum yield of oil (Y_m, kg ha^{-1}), which corresponded to the yield in the fully irrigated treatment from the same year (Trt. 1, Table 1). $1-Y_a/Y_m$ and Y_a/Y_m were related to $S_{d,i}$ and the temperature sum from growth start in spring ($t_{s,i}$, °Cd) by Eqs. (2) and (3), respectively:

$$\left(1 - \frac{Y_a}{Y_m}\right) = \sum_{i=1}^{n} S_{d,i}\left(a + a_1 t_{s,i} + a_2 t_{s,i}^2 + a_3 t_{s,i}^3 + a_4 t_{s,i}^4\right) \qquad \mathbf{2}$$

$$\frac{Y_a}{Y_m} = \prod_{i=1}^{n}\left[1 - S_{d,i}\left(a + a_1 t_{s,i} + a_2 t_{s,i}^2 + a_3 t_{s,i}^3 + a_4 t_{s,i}^4\right)\right] \qquad \mathbf{3}$$

where i is a day number between growth start in spring and harvest. In Eqs. (2) and (3) $S_{d,i}$ quantifies the stress level at the i'th day and the polynomial part describes the relative yield decrease caused by one stress-day as a function of temperature sum i.e. crop development. Relative yield decrease caused by one stress-day we will term the drought sensitivity at a given temperature sum. In the linear statistical model Eq. (2) the parameters were estimated from the data by the linear procedure REG of SAS (SAS Institute, 1988) while the parameters of the multiplicative model in Eq. (3) were estimated by the non-linear least-squares iterative procedure NLIN. In the same way relative oil concentration of the seeds (O_a/O_m), relative number of seeds per unit area (N_a/N_m) and relative interception of PAR by green crop parts during the pod-filling phase (I_a/I_m) were related to stress-level and crop development.

Results and discussion

The hypothesis that oil yield was linearly related to aboveground biomass was tested on the 1991-1994 data and could be rejected (Fig. 1), as we found a highly significant effect of treatment ($P < 0.001$) on this relationship in 1992, 1993 and 1994. This indicated that the oil yield did not have a uniform drought sensitivity during the growing season and therefore probably was affected by other physiological reactions to drought than decrease in photosynthesis and transpiration. The root mean square error (RMSE) for the overall linear relationship of 209 kg ha-1 (Fig. 1) also showed that even if biomass

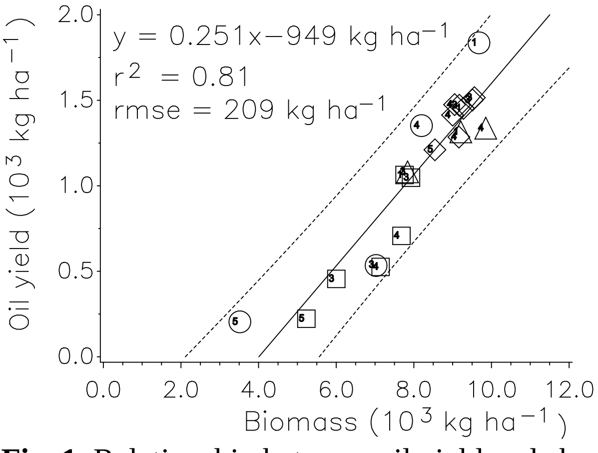

Fig. 1. Relationship between oil yield and aboveground biomass. The stippled lines gives the limits in a 95 % confidence interval for a new individual predicted value. Each point is the mean of four measurements.

could be predicted with good accuracy from transpiration, oil yield could not be precisely estimated from transpiration by assuming a linear relationship between oil yield and biomass. Accordingly, procedures that can improve the accuracy have to be sought.

It is probably a sound assumption that severe drought stress at any growth stage will decrease yield and therefore only positive values of the polynomial, i.e. drought sensitivity (Eqs. (2) and (3)), can be accepted. We therefore decided to fit Eqs. (2) and (3) only to data from treatments where yield was actually decreased. This diminished the number further from 45 to 22 treatments during 1982-1994. The frequency of drought incidents at different temperature sum intervals will affect the validity interval of the estimated curve. In Fig. 2. the sum of Sd in each 100 ^oCd interval from onset of growth to maturity is shown. The distribution of the sum of Sd was satisfactorily balanced from 400 ^oCd, corresponding to early flowering, until 1200 ^oCd, corresponding to near full maturity. Before flowering the data material contained a low number of Sd, indicating that the polynomial values in this area should be regarded with less confidence and reflecting that drought is quite rare under Danish condi-

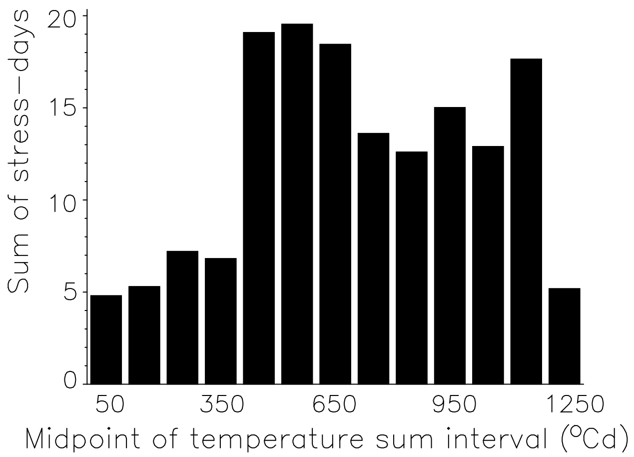

Fig. 2. Sum of stress-days in each 100 ^oCd interval from onset of growth in spring to maturity for the 22 treatments (1982-1994) used in the analysis of relative oil yield.

tions during the vegetative period. We found that the functions tended to estimate negative drought sensitivities during the vegetative phase. Slight drought during this phase may in some cases have a beneficial effect on yield by decreasing leaching of nitrogen, by decreasing the stem length and the tendency for lodging or in some other way condition the crop to drought. However, as stated above it is probably a sound assumption that severe drought stress will decrease yield. This points to a shortcoming of the models. Eqs. (2) and (3) imply that, on a given day at a given temperature sum (ts,i'), relative yield decrease is proportional to Sd,i' with a proportionality constant i.e. drought sensitivity given by the polynomial coefficients (a - a4). The same is implied for a short temperature sum interval where the drought sensitivity can change only little. This assumption of proportionality between relative yield decrease and Sd might be a gross simplification. For the vegetative period it seems that drought sensitivity was negetative for small values of Sd but probably positive for high values (cumulated over a few days). Therefore, the assumption that Sd is proportional to relative yield decrease does not hold for this period and the drought sensitivity cannot be estimated with these simple models. To avoid negative drought sensitivities we fitted the models in more steps, where *Sd* values outside the positive drought sensitivity range were set to zero until correspondence was reached with the polynomial intercept with the x-axis. Reduced forms of the temperature sum polynomials were also tested i.e. zero to fourth order.

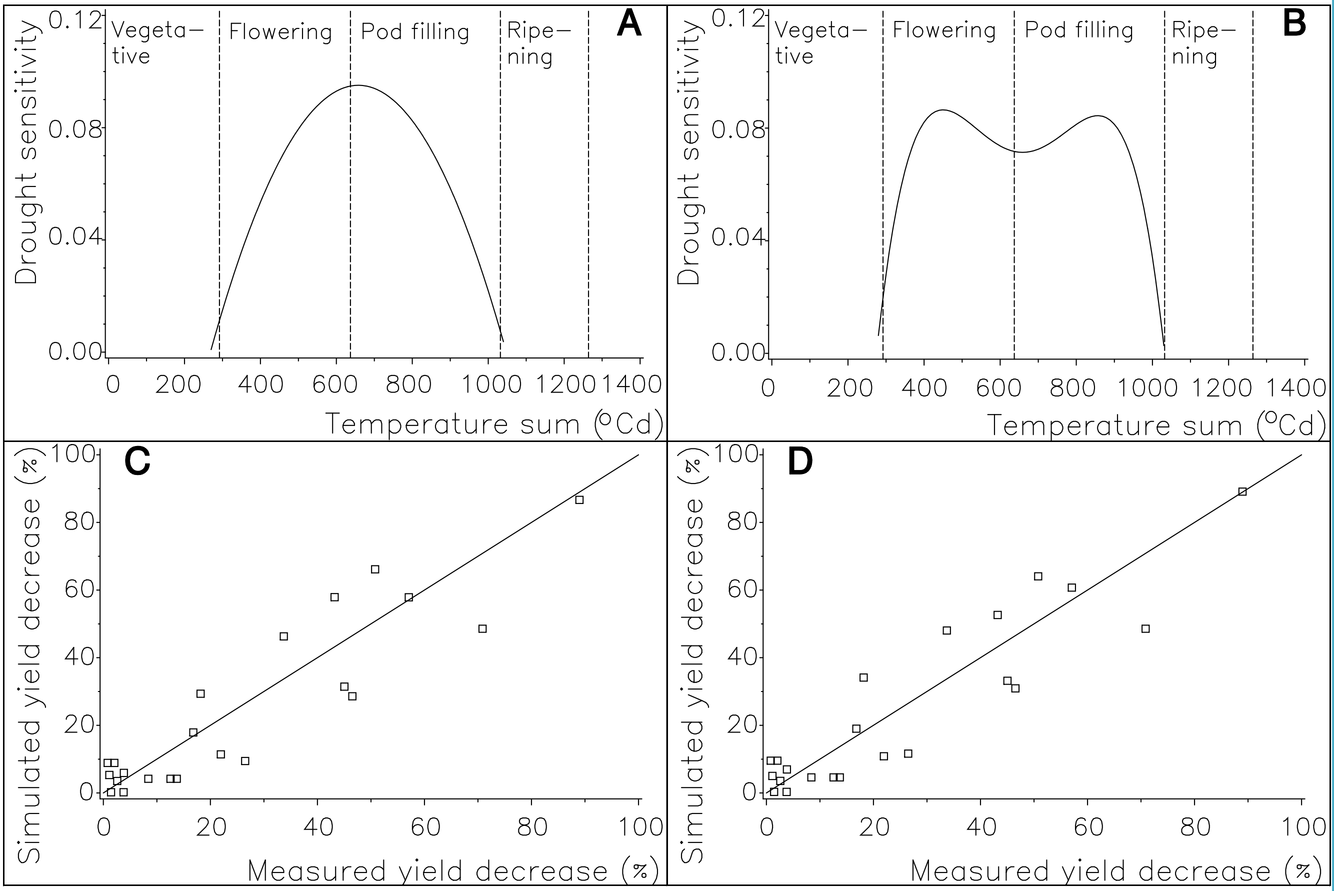

Fig. 3A-D. Relative decrease in oil yield. (**A-B**) per unit of *Sd* as a function of temperature sum from onset of growth, Eq. (3) second order polynomial and fourth order polynomial, respectively. (C-D) Simulated versus measured, respectively. The coefficients, RMSE and validity interval (Eq. (3)) were a = -1.76E-1, a1 = 8.24E-4, a2 = -6.26E-7, RMSE = 0.115, 269 °Cd < ts < 1047 °Cd and a = -1.15, a1 = 8.36E-3,
a2 = -2.05E-5, a3 = 2.16E-8, a4 = -8.23E-12, RMSE = 0.120, 276 °Cd < ts < 1031 °Cd, respectively.

The second, third and fourth orders form of the multiplicative model (Eq. (3)) gave almost the same RMSE (Fig. 3), which was lower than RMSE of the additive model (Eq. (2)). The second and fourth order polynomials of Eq. (3) are shown in Fig. 3 together with plots of simulated versus measured relative decrease in oil yield. Although, the second and fourth order polynomials do not exhibit very different numerical values of drought sensitivity at any temperature sum, they are qualitatively very different since the latter shows two maxima of drought sensitivity, one in the middle of the flowering phase of c. 8.6% and another quite late in the pod-filling phase of c. 8.4%. We will return to this point in the analysis of yield components. From the two polynomials in Fig. 3 it is seen that maximum drought sensitivity occurred between mid-flowering and the beginning of pod-filling where yield loss per unit of Sd amounted to 8.5-9.5%. It can also be noted that the drought sensi¬tivity varied strongly within the defined growth phases, which does not coincide with the assumption that the drought sensitivity is constant for each growth phase.

Mogensen (1980) concluded for spring barley that a stress-day could be regarded as a day without production. However, the sensitivity of 8.5-9.5% found here for oilseed rape clearly exceeded the oil production that can be achieved in one day. Similarly, Andersen & Aremu (1991) concluded that a maximum drought sensitivity of 11.6% found for seed yield of peas during flowering exceeded the maximum daily production rate.

We fitted Eqs. (2) and (3) to data for O_a/O_m during 1982-1994, N_a/N_m during 1991-1994 and I_a/I_m during 1991-1994. In Fig. 4 the resulting polynomials for N_a/N_m and I_a/I_m are shown, together with simulated versus measured relative decrease in the size of components. Table 2 gives the derived parameters in the polynomials and RMSE for the models. For the decrease in relative oil concentration per unit of *Sd* no relation to the developmental stage could be ascertained and the decrease was therefore modelled simply as proportional to the accumulated number of Sd. The oil concentration was negatively correlated with the nitrogen concentration of the seeds (Andersen et al., 1996) and may therefore be explainable not only from number of *Sd* and developmental stage.

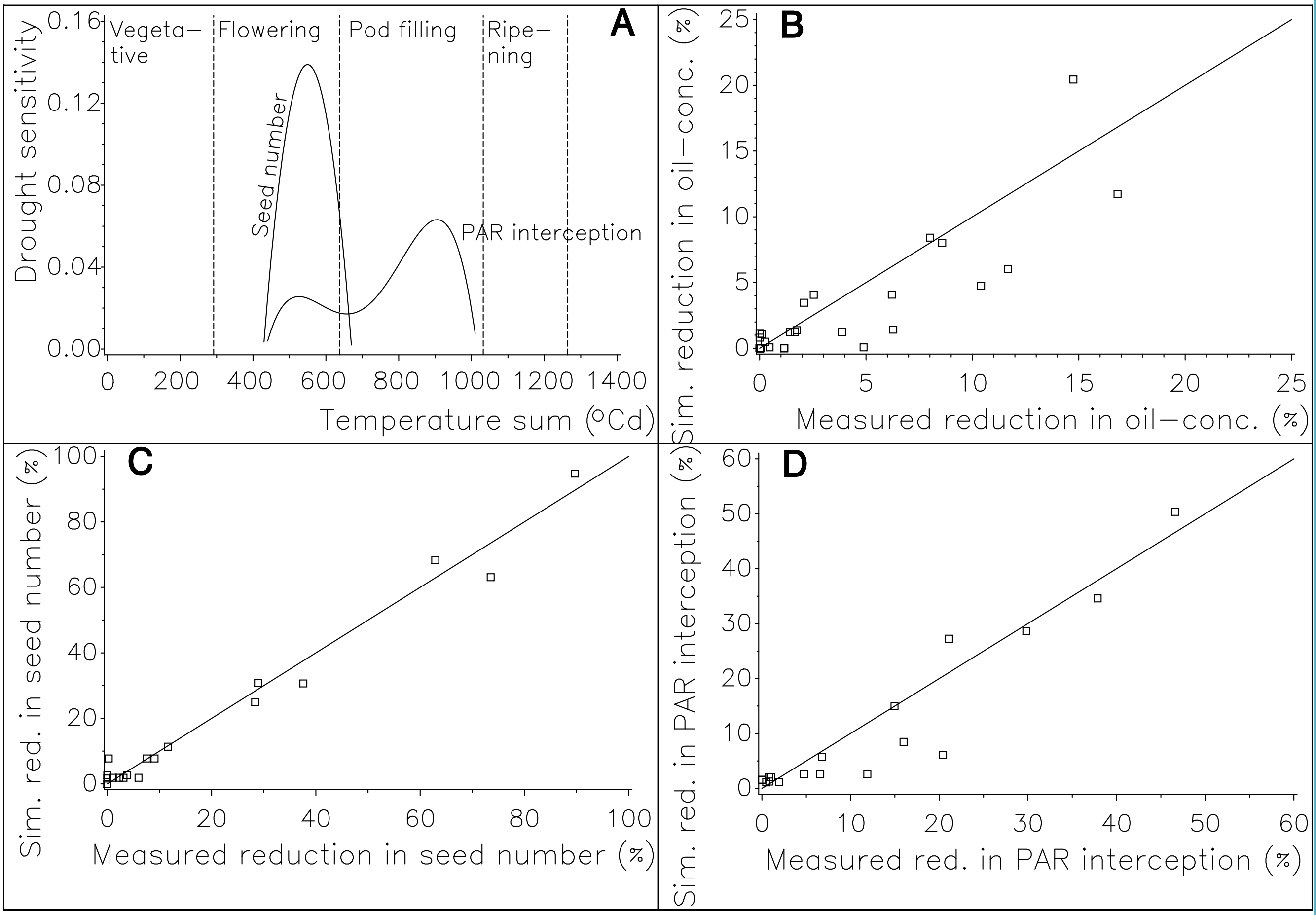

Fig. 4A-D. Relative decrease in oil-concentration, seed number and PAR interception. (**A**) per unit of *Sd* as a function of temperature sum from onset of growth (oil-conc. not shown). (**B-D**) Simulated versus measured. Coefficients and validity interval of polynomials and RMSE of models are given in Table 2.

From Fig. 4A it is seen that maximum drought sensitivity of seed number per unit area occurred in the flowering phase when drought sensitivity of seed number was very high, c. 13.9% reduction per unit of *Sd*. The reduction in seed number was about equally attributable to a reduced number of pods and a reduced number of seeds per pod (Andersen et al., 1996). In treatments that were drought stressed during flowering up to 80% of the seed primordia were aborted and the model gave a close fit to these data (Fig. 4C). However, the adverse effect of this on seed and oil yield was partly compensated by a higher seed weight in these treatments. In 1991, 1992 and 1993, when moderate to severe drought occurred during the flowering phase, seed weight was increased with 25 - 34% compared to fully irrigated (Andersen et al., 1996). If this compensation of c. 30% is taken into account the relative effect on economic yield from seed abortion may be estimated as 70% of 13.9% or 9.8% decrease per unit of Sd, which is slightly higher than the 8.6% estimated earlier. However, as there seemed to be a good proportionality between number of *Sd* and the relative decrease in seed number at a given temperature sum, and if there is an upper limit of about 30% to the compensation in seed weight, then there cannot be a good proportionality between relative decrease in economic yield and the number of *Sd* again pointing to the shortcomings of the models as mentioned for the vegetative period. For instance if more than 30% of the seed were aborted, we would expect the subsequent units of *Sd* to have full impact on economic yield, i.e. 13.9% reduction, while small reductions in seed number may be fully compensated by a higher seed weight. Therefore the drought sensitivity of economic yield may be assumed to increase initially with accumulated Sd during the flowering phase. This might to some extent explain the poorer fit to data in Fig. 3C,D than in Fig. 4C.

Table 2. Estimated parameters a, a_1, a_2, a_3 and a_4 in the drought sensitivity polynomials. RMSE is the standard error of regression on $1\text{-}O_a/O_m$ (n=24), $1\text{-}N_a/N_m$ (n=17) and I_a/I_m (n=18) . The validity intervals, i.e. the intercepts with the x-axis, were from t_s = 429 to t_s = 670 °Cd for $1\text{-}N_a/N_m$, and from t_s = 435 to t_s = 1015 °Cd for I_a/I_m.

Dependent variable	a	a_1	a_2	a_3	a_4	RMSE
$1\text{-}O_a/O_m$ (Eq. 2)	7.07E-3	0.0	0.0	0.0	0.0	0.029
$1\text{-}N_a/N_m$ (Eq. 2)	-2.72	1.04E-2	-9.46E-6	0.0	0.0	0.048
I_a/I_m (Eq. 3)	-3.59	2.23E-2	-5.04E-5	4.95E-8	-1.78E-11	0.053

Andersen et al. (1996) found that, in fully irrigated treatments, seed yield converted to carbohy¬drate equivalents was proportional to PAR interception during the pod-filling phase with a conversion factor of 2.47 g MJ-1, which was almost equivalent to the overall conversion factor of 2.38 g MJ-1 between biomass and PAR interception for the whole season. Thus, all assimilates formed during the pod-filling phase seemed to be incorporated in seeds. However, when seed number was reduced owing to drought during flowering, the proportion of assimilates incorporated in the seeds was reduced and more ended up in the straw fraction. Andersen et al. (1996) hypothesized that this indicated a sink strength limitation, the seeds reaching a maximum size. Further analysis, where about 500 seeds from each plot in 1992 were weighed individually, however, showed that the variance of the seed size distribution did not deviate between treatments. This indicated that the inefficient incorporation of assimilates might alternatively be explained by a less efficient translocation of assimilates to seeds from stem and leaf parts than from the pool of assimilates fixed by pod walls. Since pod number was reduced by drought during flowering a smaller proportion of PAR was intercepted by pod walls compared to stem and leaf parts in those treatments. Sheoran et al. (1991) showed for B. campestris that the translocation of assimilates to seeds inside pods shaded by aluminium foil was small, since seeds reached less than 30% of the weight found in non-shaded pods. In their study most of the carbon for seed growth came from pod wall fixation.

We conclude that abortion of pod and seed primordia was the most important physiological process leading to reduced yield in oilseed rape exposed to drought stress.

Investigations into a number of other crop plants have pointed to three possible causes of this abortion process, namely a lack of assimilate supply to the seed primordia (e.g. Boyle et al., 1991), a hormonal signal produced in the root system (Kobata et al., 1994) or exposure of the seed primordia to lethal low water potential (Zinselmeier et al., 1995). These possibilities deserve further attention in order to analyse if seed abortion can be diminished by selecting favourable genetic traits.

The drought sensitivity of PAR interception during pod-filling (Fig. 4A) had two maxima, the first during flowering of c. 2.6% and the second in late pod-filling of c. 6.3%. The first maximum coincided with that for seed number and was probably associated with the reduction in number and green area index of pods. The second maximum was most likely caused by accelerated senescence of the pod canopy during drought. Also this model gave quite a close fit to the data. Andersen et al. (1996) found that even when drought stress was severe during the pod-filling phase, the photosynthetic efficiency of the pod canopy was almost maintained, i.e. the PAR interception to seed yield conversion factor was almost 2.47 g MJ-1 as in fully irrigated treatments. This indicated that Ia/Im was a good estimator of relative seed size and Ya/Ym if seed number was not reduced by drought during flowering. Therefore, the second maximum of the drought sensitivity of oil yield of c. 8.4% at a temperature sum of c. 900 ^{o}Cd (Fig. 3B) may largely be explained by the drought sensitivity of PAR interception of c. 6.3% at almost the same temperature sum. Finally, when comparing the polynomial in Fig. 3B with those in Fig. 4A, we would expect the local minimum at temperature sum c. 700 oCd (Fig. 3B) to be lower. It might be that the previously mentioned shortcomings of the yield model, i.e. lack of proportionality between Sd and Ya/Ym during flowering, caused the effects of drought stress to be overvalued during this period or that effects that have not been fully evaluated in this treatment, e.g. decrease in photosynthetic efficiency, are especially pronounced during this stage.

In conclusion, we have developed a simple mathematical expression for the drought sensitivity of oil yield of winter oilseed rape as a continuous function of crop development, and analysed it in terms of the major physiological reactions leading to decreased yield during drought. These reactions include seed abortion and senescence of the pod canopy but not photosynthesis per se, and can to a large extent explain the variation during the crop's life cycle in drought sensitivity, which showed two maxima, one at mid-flowering and a second at late pod-filling. Despite the shortcomings of some assumptions behind the mathematical expression leading to variation between measured and predicted relative yield, we find it suitable for inclusion in decision support systems for the prediction of yield response to irrigation based on soil water balance modelling and meteorological weather forecasts as in the MARKVAND system (Plauborg et al., 1996).

References

Andersen A (1986) Root growth in different soil types. Tidsskr. Planteavl Report S-1827, Statens Planteavlsforsøg, Copenhagen.

Andersen MN, Aremu JA (1991) Drought sensitivity, root development and osmotic adjustment in field grown peas. Irrig Sci 12: 45-51.

Andersen MN, Jensen CR, Lösch R (1992) The interaction effects of potassium and drought in field-grown barley. I. Yield, water-use efficiency and growth. Acta Agric. Scand., Sect. B 42: 34-44

Andersen MN, Heidmann T, Plauborg F (1996) The effects of drought and nitrogen on light interception, growth and yield of winter oilseed rape. Acta Agric. Scand., Sect. B, Soil and Plant Sci. 46: 55-67
Bierhuizen JF, Slatyer O (1965) Effects of atmospheric concentration of water vapour and CO2 in determining transpiration-photosynthesis relationship of cotton leaves. Agr. Meteorol. 2: 259-270
Boyle MG, Boyer JS, Morgan PW (1991) Stem infusion of liquid culture medium prevents reproductive failure of maize at low water potential. Crop Sci. 31: 1246-1252
de Wit CT (1958) Transpiration and crop yields. Versl. Landbouwk. Onderz. 64.6 Inst. of Biol. and Chem. Res. on Field Crops and Herbage, Wageningen, The Netherlands
Doorenbos J, Kassam AH (1979) Yield response to water. FAO Irrigation and Drainage Paper No. 33. FAO, Rome
Hansen L (1976) Jordtyper ved statens forsøgsstationer. Tidsskr. Planteavl 80: 742-758
Hansen S, Storm B, Jensen HE (1986) Spatial variability of soil physical properties. Theoretical and experimental analyses. I. Soil sampling, experimental analyses and basic statistics of soil physical properties. Department of Soil and Water and Plant Nutrition, The Royal Veterinary and Agricultural University, Copenhagen
Hiler EA, Clark RN (1971) Stress day index to characterize effects of water stress on crop yields. Trans. ASAE 14: 757-761
Hiler EA, Howell T (1983) Irrigation options to avoid critical stress: An overview. In: Taylor HM, Jordan WR, Sinclair TR (eds) Limitations to Efficient Water Use in Crop Production. ASA-CSSA-SSSA, Madison, WI, p 479-497
Howell TA (1990) Relationships between crop production and transpiration, evapo-transpiration, and irrigation. In: Steward BA, Nielsen DR (eds) Irrigation of Agricultural Crops. ASA-CSSA-SSSA, Madison, WI, p 391-434
Jensen F (1986) Irrigation of spring rape and winter rape. Tidsskr. Planteavl 90: 251-258
Kanemasu ET (1983) Yield and water use relationships: Some problems of relating grain yield to transpiration. In: Taylor HM, Jordan WR, Sinclair TR (eds) Limitations to Efficient Water Use in Crop Production. ASA-CSSA-SSSA, Madison, WI, p 413-417
Kobata T, Tanaka S, Utumi M (1994) Sterility in rice (Oryza sativa L.) subject to drought during the booting stage occurs not because of lack of assimilate or of water deficit in the shoot but because of dehydration of the root zone. Jpn. J. Crop Sci. 63: 510-517
Mikkelsen HE, Olesen JE (1991) Sammenligning af metoder til bestemmelse af potentiel vandfordampning. Tidsskr. Planteavl Report S-2157, Statens Planteavlsf¬orsøg, Copenhagen
Mogensen VO (1980) Drought sensitivity at various growth stages of barley in relation to relative evapotranspiration and water stress. Agron. J. 72: 1033-1038
Mogensen VO, Jensen HE, Abdur Rab M (1985) Grain yield, yield components, drought sensitivity and water use efficiency of spring wheat subjected to water stress at various growth stages. Irrig. Sci. 6: 131-140
Nielsen JD, Møberg JP (1985) Klassi¬ficering af jordprofiler fra forsøgsstationer i Danmark. Tidsskr. Planteavl 89: 157-167
Olesen JE, Plauborg F (1992) MVTOOL version 1.10 for developing MARKVAND. SP Report No. 27 1995. Danish Institute of Plant and Soil Science, Research Centre Foulum
Penman HL (1956) Evaporation: an introductory survey. Neth. J. Agric. Sci. 4: 4-29
Petersen C, Jørgensen U, Svendsen H, Hansen S, Jensen HE, Nielsen NE (1995) Parameter assess¬ment for simulation of biomass production and nitrogen uptake in winter rape. Europ. J. Agron. 4: 77-89

Plauborg F, Andersen MN, Heidmann T, Olesen JE (1996) Markvand: A decision support system for irrigation scheduling. In: Camp CR, Sadler EJ, Yoder RE (eds) Evaporation and Irrigation Scheduling. Proceedings of the International Conference, Nov. 3-6, 1996, San Antonio, Texas. ASAE. p 527-535
Sheoran IS, Sawhney V, Babbar S, Singh R (1991) In vivo fixation of CO2 by attached pods of Brassica campestris L.. Ann. Bot. 67: 425-428
SAS Institute (1988) SAS/STAT. Users Guide, Release 6.03 Edition. SAS Institute, Cary, NC
Tanner CB, Sinclair TR (1983) Efficient water use in crop production: Research or re--search. In: Taylor HM, Jordan WR, Sinclair TR (eds) Limitations to Efficient Water Use in Crop Production. ASA-CSSA-SSSA, Madison, WI, p 1-27
Zinselmeier C, Westgate ME, Schussler JR, Jones RJ (1995) Low water potential disrupts carbohydrate metabolism in maize (Zea mays L.) ovaries. Plant Physiol. 107: 385-391

Synthesis on Crop Water Production Functions

A total of 12 crops have up to now been included in the ‘yield response to irrigation’ model (Table 1). Most of these (apart from fodder beet) gave the best fit to data when using the non-linear or multiplicative model (Eq. 3). Most of the crops display a top in drought sensitivity around flowering time (Figs. 2, 3, 4) indicating that the reproductive physiological processes are the most sensitive to drought. However, a contributing factor might be that a stress-day at high evaporative demand have more impact on yield than at low reference-evapotranspiration conditions. In general the model fit was good with RMSE values from 3 to 14 % of the relative yield decrease that vary from 0-100 %.

Table 1. Parameters in the drought sensitivity polynomial (Eqs. 2 and 3) for 12 crops derived from irrigation experiments at Jyndevad Experimental Station. Number of observations (n) and validity interval from Tb to Te in degree days.

Mtype	Crop	a0	a1	a2	a3	a4	RMSE	n	Tb	Te
NLIN	Winter barley	-7.77E-02	5.32E-04	-4.52E-07	0	0	0.14	9	171	1004
NLIN	Spring barley	-9.27E-02	2.83E-04	-1.51E-07	0	0	0.11	25	424	1451
NLIN	Winter wheat	-7.44E-05	1.20E-04	-7.26E-08	0	0	0.09	43	1	1656
NLIN	Potatoes, midl.	5.19E-03	8.71E-05	-6.11E-08	0	0	0.05	26	0	1482
NLIN	Winter rape	-1.15	8.36E-03	-2.05E-05	2.16E-08	-8.3E-12	0.11	26	276	1031
NLIN	Spring rape	-7.08E-02	2.78E-04	-1.56E-07	0	0	0.09	37	309	1472
NLIN	Peas	-1.38E-01	8.26E-04	-9.82E-07	3.26E-10	0	0.07	44	220	1226
NLIN	Rye grass	1.34E-02	8.46E-06	-7.04E-09	0	0	0.03	14	0	2106
Reg	Fodder beet	-5.66E-02	6.66E-05	-7.74E-09	0	0	0.06	15	957	2594
NLIN	Maize	0.00438	4.71E-05	-0.3E-07				31		
NLIN	RedCloverGrass	0.018966	-1.35E-05	3.00E-09	0	0				
NLIN	Potatoes, late	-1.30E-01	4.01E-04	-1.91E-07	0.00E+00	0			403	1694

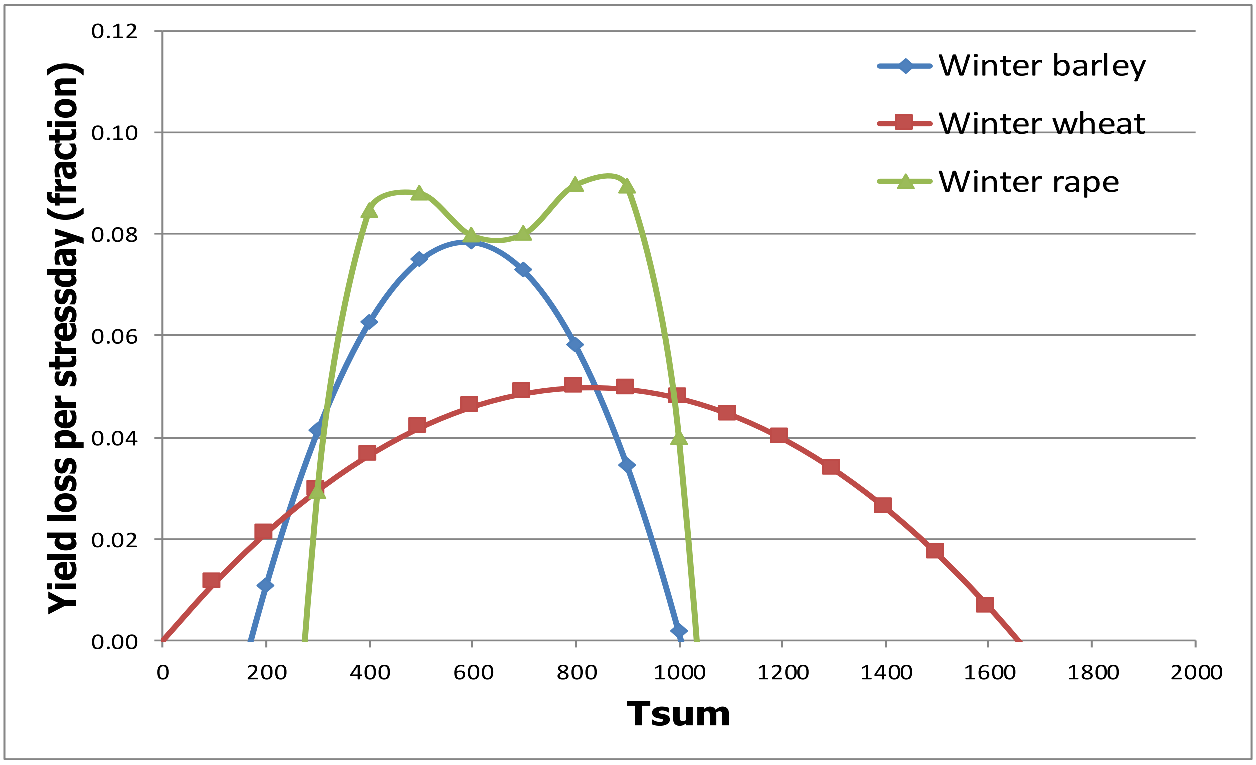

Figure 2. Drought sensitivity of winter sown crops over the season based on experimental data from irrigation trials at Jyndevad.

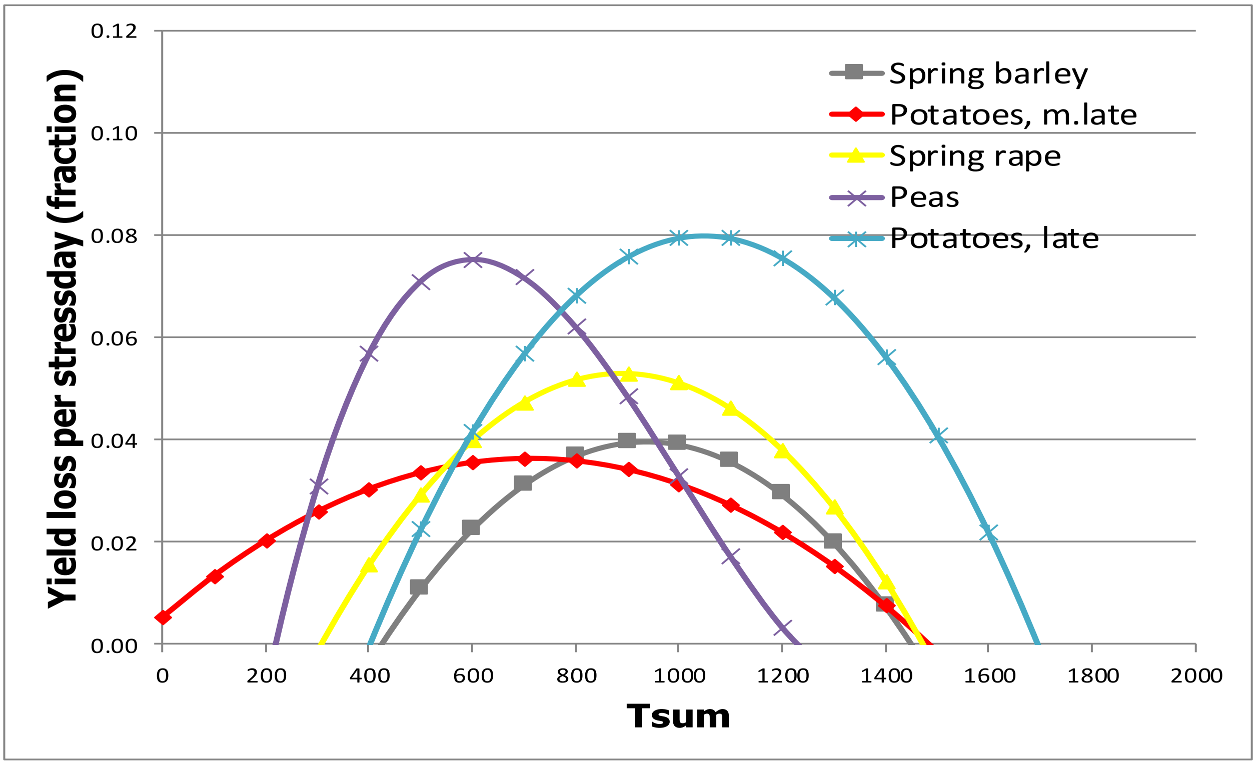

Figure 3. Drought sensitivity of spring sown crops over the season based on experimental data from irrigation trials at Jyndevad.

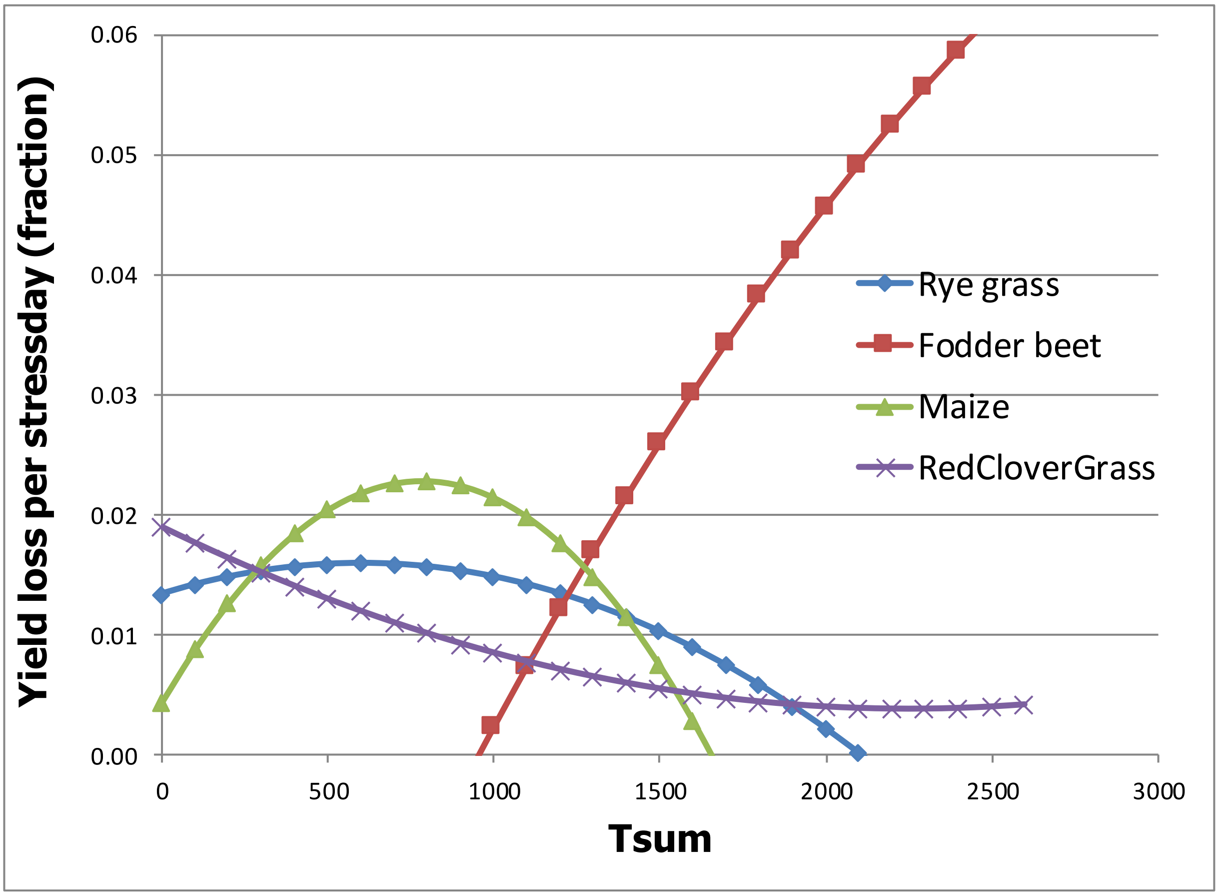

Figure 4. Drought sensitivity of fodder crops over the season based on experimental data from irrigation trials.

References

Andersen, M.N. & Aremu, J.A. 1991. Drought sensitivity, root development and osmotic adjustment in field grown peas. Irrig. Sci. 12, 45-51.

Andersen, M.N., Jensen, C.R. & Lösch, R. 1991. Derivation of pressure-volume curves by a non-linear regression procedure and determination of apoplastic water. J. Exp. Bot. 42, 159-165.

Andersen, M.N. 1992. Organisering af data fra vandingsforsøg. Arbejdsnotat nr. 12. Afdeling for Kulturteknik. Forskningscenter Foulum. 46 pp.

Andersen, M.N., Jensen, C.R. & Lösch, R. 1992. The interaction effects of potasssium and drought in field-grown barley. I. Yield, water-use efficiency and growth. Acta Agric. Scand., Sect B 42, 34-44.

Brown, K.F., Messem, A.B., Dunham, R.J. & Biscoe, P.V. 1987. Effect of drought on growth and water use of sugar beet. J. Agric. Sci. Camb. 109, 421 435.

Hansen, L. 1976. Jordtyper ved statens for-søgsstationer. Tidsskr. Planteavl 80, 742-758.

Hansen, S., Storm, B. & Jensen, H.E. 1986. Spatial variability of soil physical properties. Theoretical and experimental analyses. I. Soil sampling, experimental analyses and basic statistics of soil physical properties. Department of Soil and Water and Plant Nutrition, The Royal Veterinary and Agricultural University, Copenhagen. 84 pp.

Hansen, S., Jensen, H.E., Nielsen, N.E. & Svendsen, H. 1990. DAISY - Soil Plant Atmosphere System Model. NPo-forskning fra Miljøstyrelsen Nr A10. 272 pp.

Heidmann, T. 1989. Startkarakterisering af arealer til systemforskning. II. Resultater fra arealet ved Foulum. Tidsskr. Planteavl, Beretning S-2007, 186 pp.

Howell, T.A. 1990. Relationships between crop production and transpiration, evapotranspi-ration, and irrigation. In: Steward, B.A. & Nielsen, D.R. (eds.). Irrigation of Agricultural Crops. ASA-CSSA-SSSA, Madison, WI, 391-434.
Jensen, C.R., Svendsen, H., Andersen, M.N. & Lösch, R. 1993. Use of the root contact concept, an empirical leaf conductance model and pressure-volume curves in simulating crop water relations. Plant Soil 149, 1-26.
Mogensen, V.O. 1980. Drought sensitivity at various growth stages of barley in relation to relative evapotranspiration and water stress. Agron. J. 72, 1033-1038.
Mogensen, V.O., Jensen, H.E. & Abdur Rab, M. 1985. Grain yield, yield components, drought sensitivity and water use efficiency of spring wheat subjected to water stress at various growth stages. Irrig. Sci. 6, 131-140.
Nielsen, J.D. & Møberg, J.P. 1985. Klassificering af jordprofiler fra forsøgsstationer i Danmark. Tidsskr. Planteavl 89, 157-167.
Olesen, J.E. 1992. MVTOOL version 1.00. A tool for developing MARKVAND. AJMET arbejdsnotat nr. 30. Afdeling for Jordbrugsmeteorologi, Forskningscenter Foulum, 44 pp.
Plauborg, F. & Olesen, J.E. 1991a. Udvikling og validering af modellen MARKVAND til vandingsstyring i landbruget. Tidsskr. Planteavl Beretning S-2113, 103 pp.
Plauborg, F. & Olesen, J.E. 1991b. MARKVAND. Vandingsstyring på PC. Grøn Viden, Landbrug, nr. 76. Statens Planteavlsforsøg, Lyngby. 4 pp.
SAS Institute. 1988. SAS/STAT Users Guide, Release 6.03 Edition. Cary, NC, pp. 1028.
Thomsen, A. & Andersen, M.N. 1991. Måling af jordens vandindhold. Tidsskr. Planteavl, Beretning S-2112, p. 79-94.
Turner, N. 1988. Measurement of plant water status by the pressure chamber technique. Irrig. Sci. 9, 289-308.

Potential yield response to irrigation

Mathias N. Andersen and Loraine ten Damme

Introduction

The extraordinary dry summer of 2018 have again raised the interest and questions about the economic benefits of establishing and investing in irrigation facilities. At present, irrigation is concentrated to the coarse textured sandy soils mainly found in western and southern part of Jutland, but on nearly all soil types farmers experienced yield losses due to drought in the summer of 2018. However, establishing irrigation facilities is expensive and has to pay back over a longer period of time. Therefore, it is absolutely crucial for the individual farmer to be able to estimate the economic gain that can be achieved given the local climate and soil type as well as crop rotation. The last estimation of this kind for Denmark was done in 1983 (Gregersen and Olesen, 1983) and since then new models for yield response to irrigation as described above have become available covering a larger number of crops than previously.

Data and calculations

26 years of climate data (1990-2015) from 10 locations in Denmark were used to analyse the irrigation requirement of 10 crops at 6 different rootzone capacities (ten Damme and Andersen, 2018). Here we present the relative yield response to irrigation based on yield simulations using the same data to simulate the water balance and relative yield of the unirrigated agricultural crops. Unfortunately, after completing this task we discovered a discrepancy in the simulation of the stress-day variable by the Vandregnskab model vis-à-vis previous simulations with the MVTOOL model used for parameterizing the yield response functions. This resulted in too high estimates of yield reductions due to drought. Therefore, at the moment, we have only been able to simulate yield reductions by using the old yield response models from Gregersen and Olesen (1983), which should serve as a baseline for comparison and evaluation of the results of simulations with the new models.

Results and discussion

Jyndevad is a location with a relatively high amount of precipitation in a Danish context. In Fig. 1 below is shown the simulation results for 4 crops that were analysed and ordered according to years with decreasing yield loss. When comparing to Skjern (Fig. 2), which has less precipitation and Flakkebjerg (Fig. 3) with even less rainfall, it is apparent that the simulated yields are decreasing with lower rainfall. It is also apparent that yields are increasing with higher root zone capacity. When comparing the average yield for three of the crops at different root zone capacities at Jyndevad and Skjern (Fig, 4) these differences become even more conspicuous. At 60 mm of root zone capacity, the estimated yield increase for irrigation at at Skjern is appreciably higher for all three crops than at Jyndevad. Both places, however, the estimated yield response to irrigation declines rapidly with increasing root zone capacity, illustrating that it is of paramount importance to the farmer to have a good estimate of the water holding capacity of the soil and as well as the precipitation before considering to invest in irrigation facilities. The foundation for this decision will be much stronger once yield increases can be estimated for a broader range of crops.

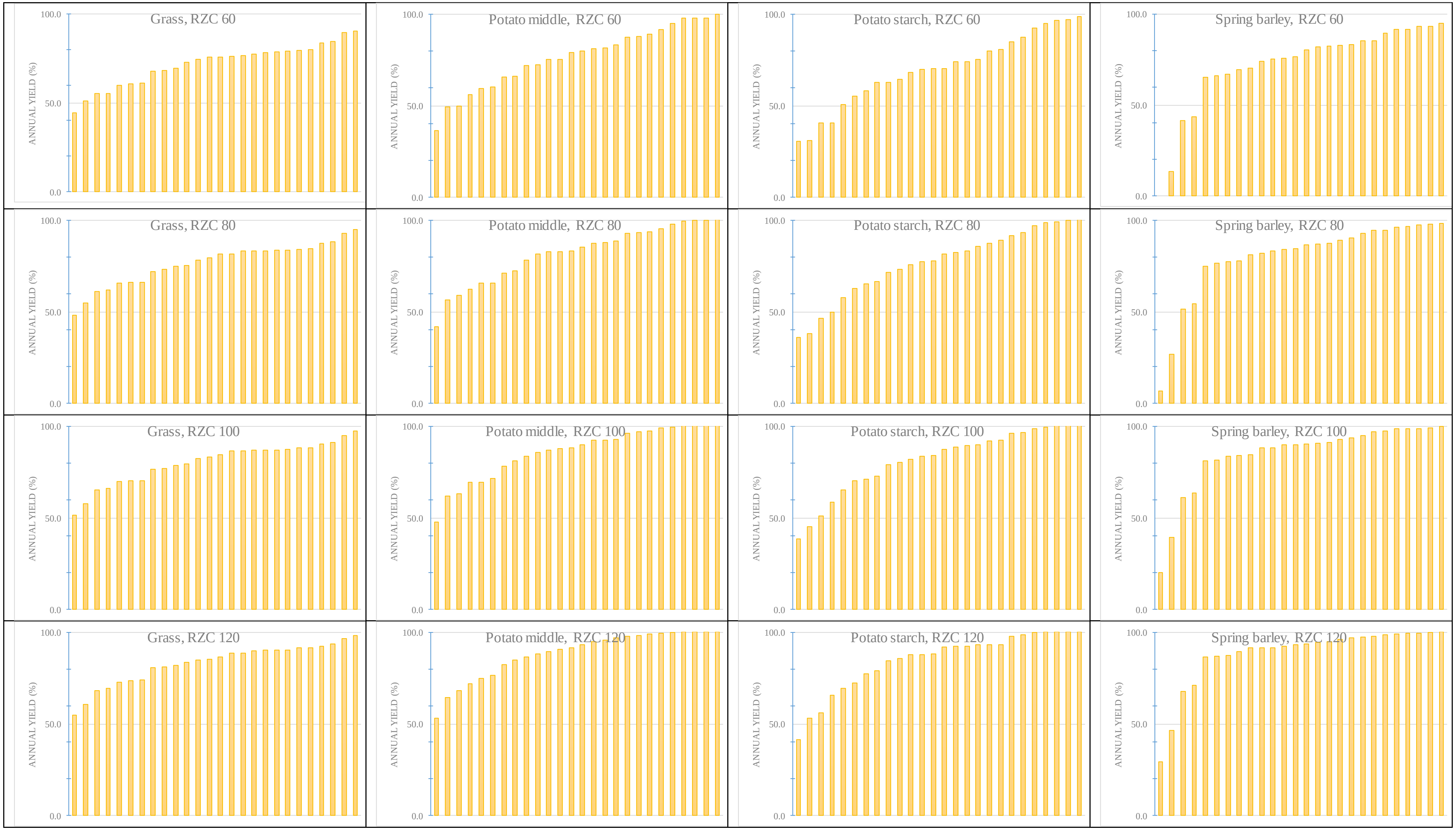
Grass, RZC 60
Potato middle, RZC 60
Potato starch, RZC 60
Spring barley, RZC 60
Grass, RZC 80
Potato middle, RZC 80
Potato starch, RZC 80
Spring barley, RZC 80
Grass, RZC 100
Potato middle, RZC 100
Potato starch, RZC 100
Spring barley, RZC 100
Grass, RZC 120
Potato middle, RZC 120
Potato starch, RZC 120
Spring barley, RZC 120
ANNUAL YIELD (%)
100.0
50.0
0.0

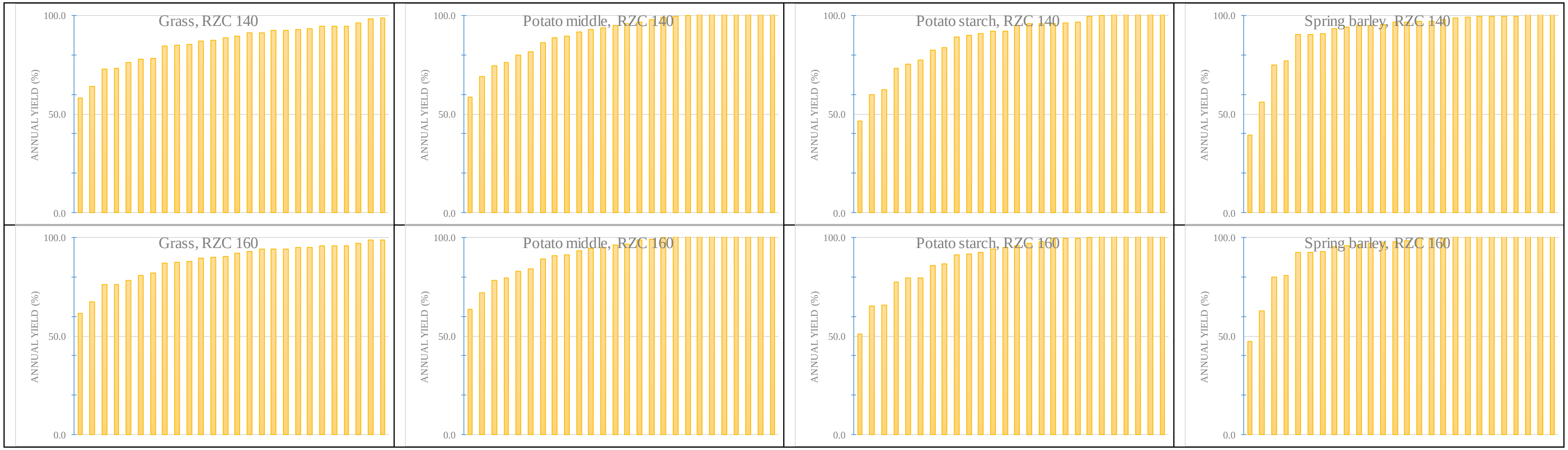

Figure 1. Relative yield of four crops simulated over a 26 year period (1990-2015) at different root zone capacities using climate data from Jyndevad and models from Gregersen and Olesen (1983)

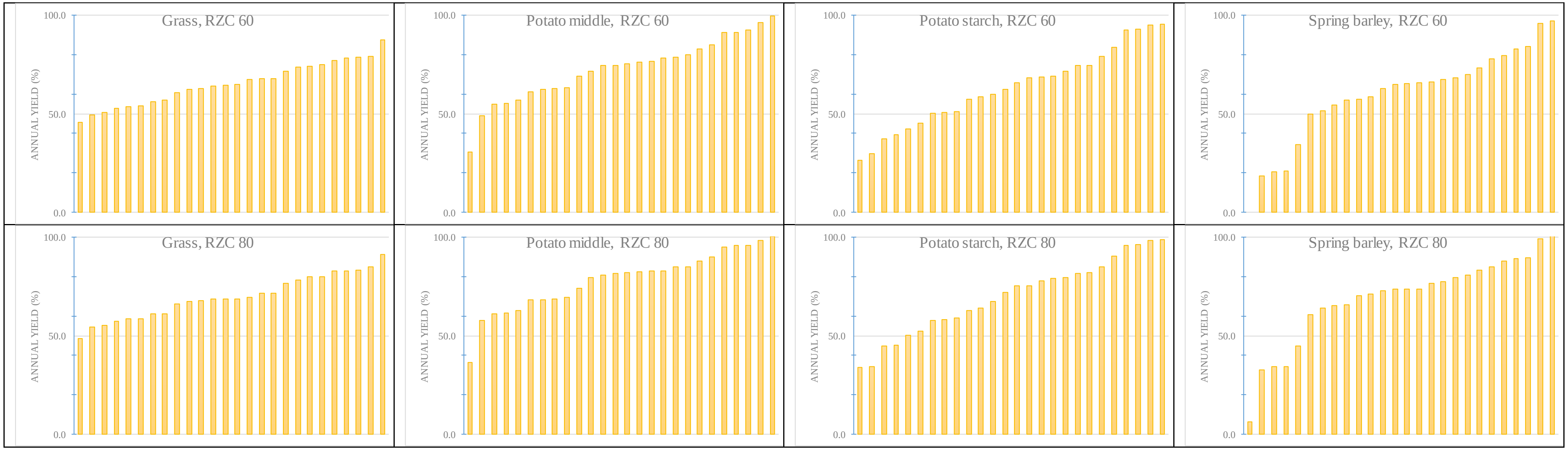

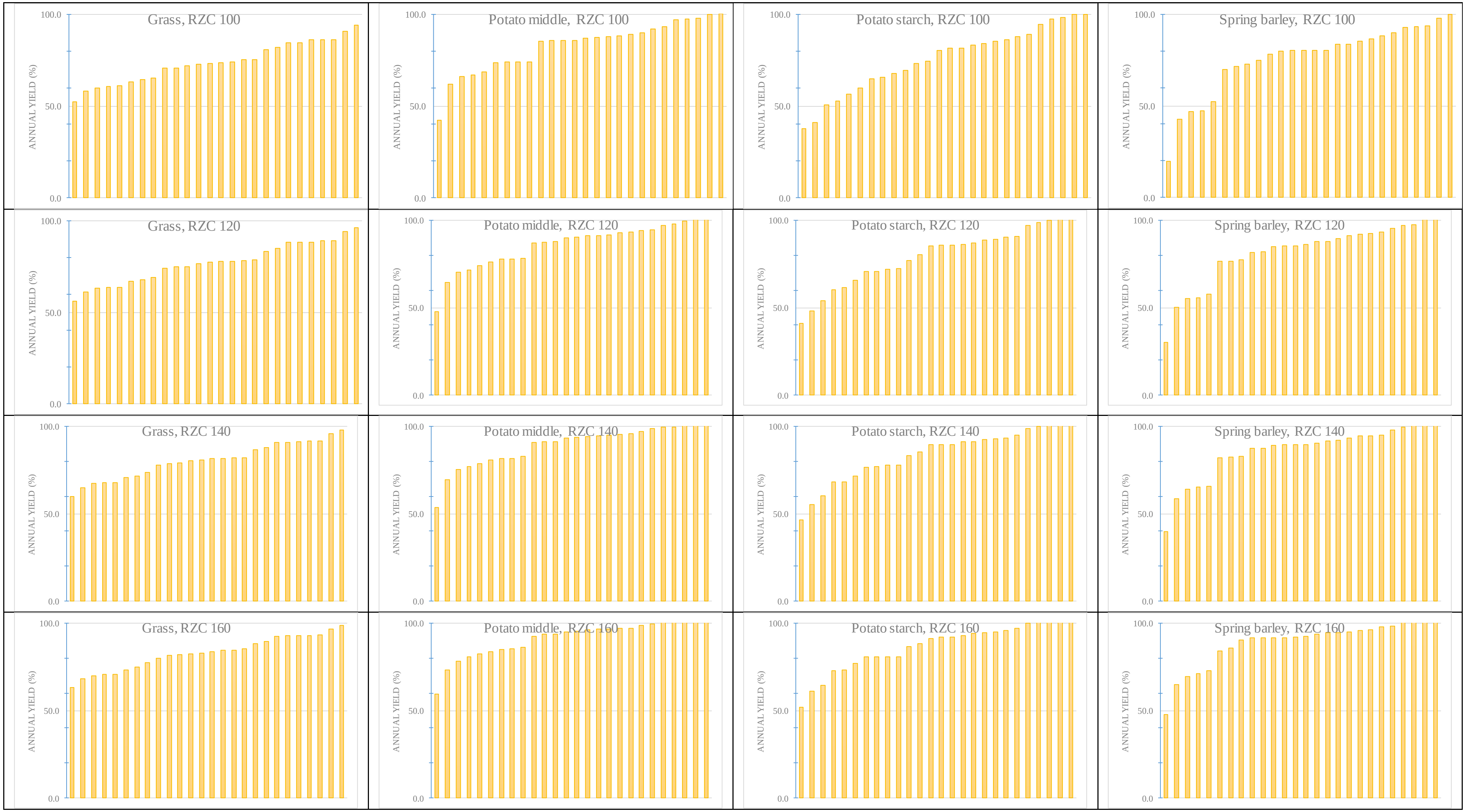

Figure 2. Relative yield of four crops simulated over a 26 year period (1990-2015) at different root zone capacities using climate data from Skjern and models from Gregersen and Olesen (1983)

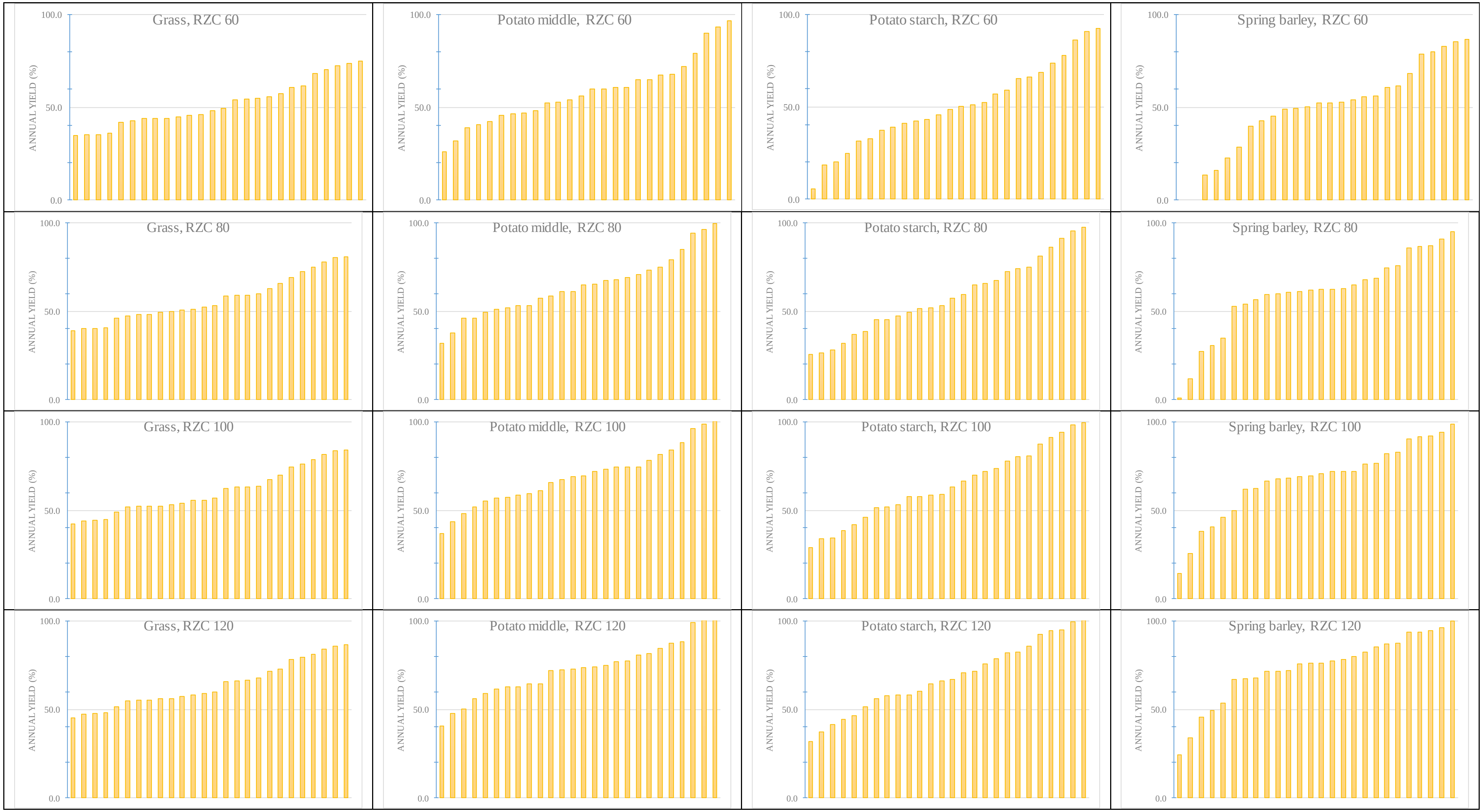
Grass, RZC 60
Potato middle, RZC 60
Potato starch, RZC 60
Spring barley, RZC 60
Grass, RZC 80
Potato middle, RZC 80
Potato starch, RZC 80
Spring barley, RZC 80
Grass, RZC 100
Potato middle, RZC 100
Potato starch, RZC 100
Spring barley, RZC 100
Grass, RZC 120
Potato middle, RZC 120
Potato starch, RZC 120
Spring barley, RZC 120
ANNUAL YIELD (%)
100.0
50.0
0.0

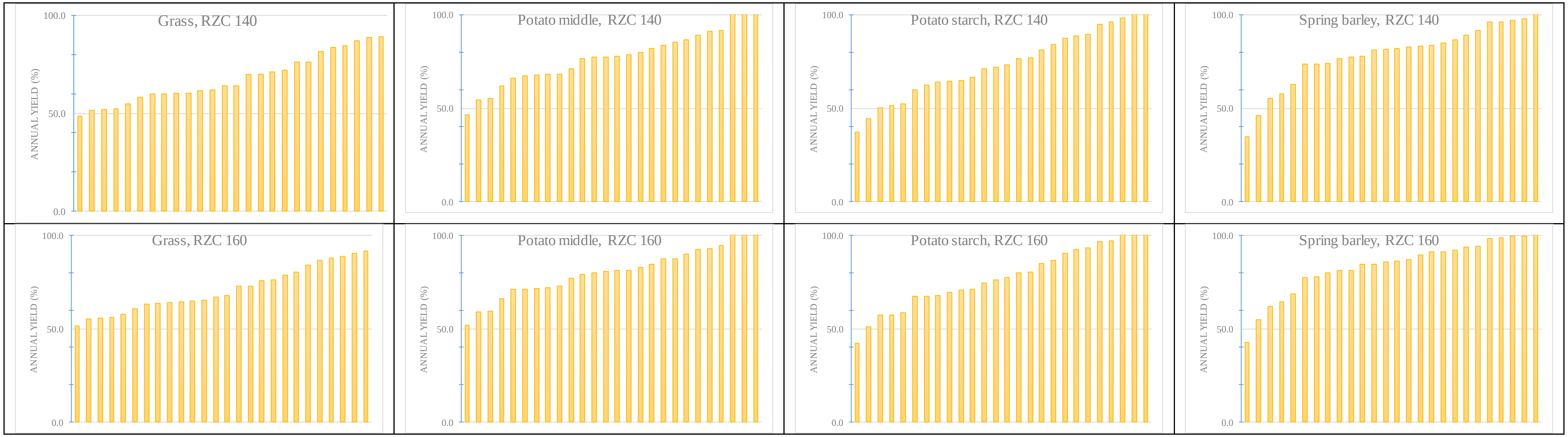

Figure 3. Relative yield of four crops simulated over a 26 year period (1990-2015) at different root zone capacities using climate data from Flakkebjerg and models from Gregersen and Olesen (1983)

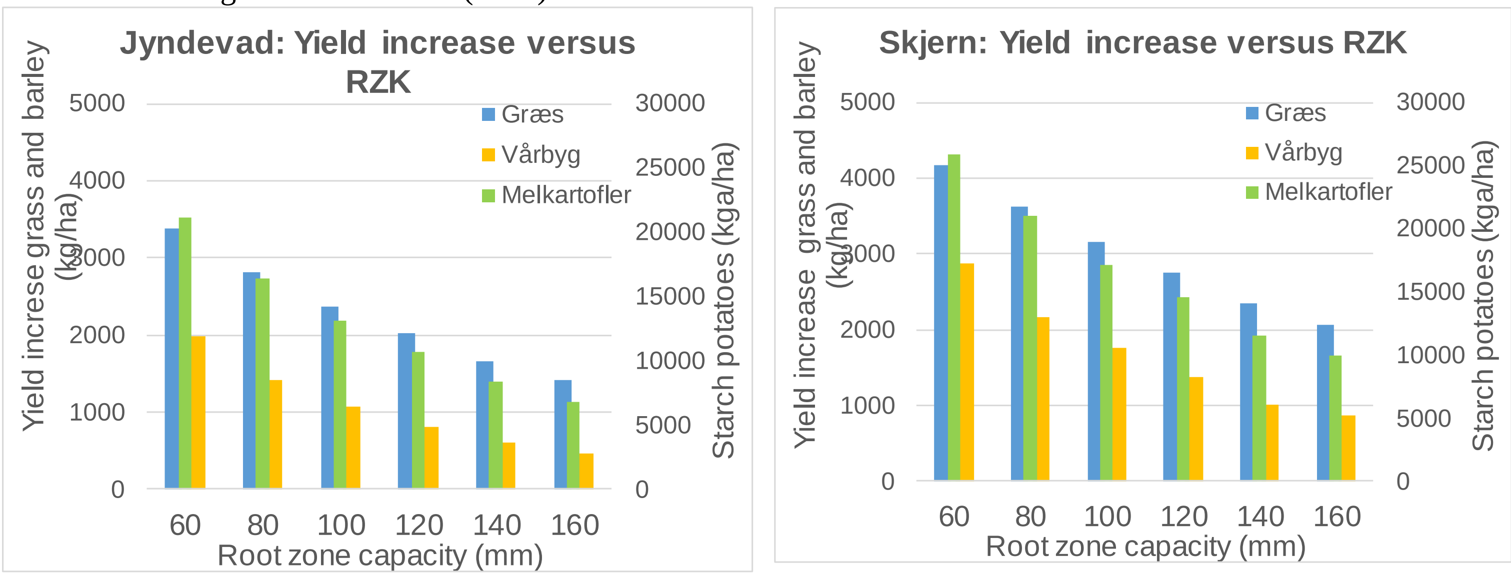

Figure 4. Relative average yield increase of three crops simulated over a 26 year period (1990-2015) at different root zone capacities using climate data from Jyndevad and Skjern and models from Gregersen and Olesen (1983).

References

Gregersen, A.K. and Olesen, J. E. 1983. Sandsynlige værdier for merudbytter ved vanding i vårbyg, græs og kartofler. Tidsskrift for Planteavl Beretning nr. S 1668. 32 pp. København.